CHARACTERIZATION OF SHORT-TERM SYNAPTIC PLASTICITY AT EXCITATORY SYNAPSES TO THE SUPRAOPTIC NUCLEUS

MICHELLE QUINLAN

CHARACTERIZATION OF SHORT-TERM SYNAPTIC PLASTICITY AT EXCITATORY SYNAPSES TO THE SUPRAOPTIC NUCLEUS

By

Michelle Quinlan

A thesis submitted to the

School of Graduate Studies in partial fulfillment of the

requirements for the degree of

Master of Science

Faculty of Medicine

Memorial University of Newfoundland

July 2006

St. John's Newfoundland

Abstract

The magnocellular neurons (MCNs) of the supraoptic nucleus (SON) synthesize and secrete the hormones oxytocin (OT) and vasopressin (AVP), which are released from the axon terminals in the neurohypophysis, as well as from the dendrites within the SON in response to physiological demand for their products. Hormone release is determined by unique firing patterns of these neurons which are dependent on intrinsic membrane properties as well as extrinsic factors such as afferent inputs. Glutamate is an important neurotransmitter in the SON, and has been shown to underlie the unique firing patterns of MCNs and to induce release of its neuropeptides. Thus, investigation of the mechanisms by which excitatory synapses to magnocellular neurons operate is critical to further our understanding of the functioning of the SON.

In the SON, a unique form of synaptic plasticity has been shown following brief, intense stimulation to the excitatory afferents. High frequency stimulation (HFS; 10-100 Hz) causes a robust increase in the frequency and amplitude of tetrodotoxin (TTX)-insensitive miniature excitatory postsynaptic currents (mEPSCs) which lasts for 5 to 20 minutes. This has been called short term potentiation (STP). Excitability of the postsynaptic cell is increased during the course of STP, suggesting that this is a physiologically relevant phenomenon. Much is yet to be determined with reference to the time course and magnitude of STP. In particular, the larger mEPSCs that appear following HFS may increase the probability of postsynaptic firing, given that the MCNs have relatively high input resistance. However, activity-dependent potentiation of mEPSC amplitude remains poorly understood. Thus, the goal of the present thesis is to better characterize STP, with particular attention to the potentiation of mEPSC amplitude.

Using a visually guided whole cell patch clamp recording technique, we confirmed that a 50 or 100 Hz, 1 sec stimulation of the excitatory afferents to MCNs resulted in both frequency and amplitude STP. These changes are dependent on extracellular calcium, since applying HFS in calcium free artificial cerebrospinal fluid had no effect on the amplitude or frequency of mEPSCs. First, we characterized the time course of STP. Both the amplitude and frequency of mEPSCs showed the most pronounced increase immediately following the stimulation. The initial frequency change was on average 30-

40 fold, which returned to baseline values with a two-exponential decay. The increase in amplitude was more modest compared to frequency (on average a 40% increase) which also decayed back gradually to baseline in most cells within 20 min.

Further, we determined if variability in basal levels of spontaneous synaptic transmission seen among the cells examined explains the variability in the magnitude of the response to stimulation. We found that baseline mEPSC frequency and amplitude were negatively related to the percentage increases following HFS, which in turn were positively related to how long the mEPSC frequency and amplitude were potentiated.

Next, we tested the hypothesis that the changes in mEPSC amplitude and frequency following HFS occur in tandem. We compared the duration of the frequency response to the duration of the amplitude response and found that they were not related: approximately half the cells tested showed longer potentiation in frequency whereas the other half had longer amplitude STP. Dissociation of these two parameters suggests that we are seeing two independent forms of synaptic plasticity. Since a similar proportion of cells showed preferential maintenance of potentiation in amplitude vs. frequency we speculated that the preference was due to the difference in phenotypes of the postsynaptic cell. However, this was not the case, as both putative oxytocin and vasopressin neurons showed both types of responses. In addition, we found that this was not a function of the intensity of stimulation, since 50 Hz and 100 Hz stimulation protocols yielded both kinds of responses. Interestingly, a high concentration of EGTA in the recording pipette to chelate postsynaptic calcium had no effect on the response of mEPSC amplitude to HFS. Addition of an NMDA receptor antagonist was also ineffective at blocking the mEPSC amplitude increase. Taken together with our observation that extracellular calcium is required for STP, these results indicate that the locus of this synaptic plasticity is presynaptic.

From here we focused on characterizing the potentiation of mEPSC amplitude. In order to do this, we took advantage of the dissociation of the time course of mEPSC amplitude and frequency. In cells that showed potentiation of mEPSC amplitude that outlasted that of mEPSC frequency, we examined larger mEPSCs that are unlikely to have resulted from random summation of multiple mEPSCs. Analysis of mEPSC waveforms (rise and decay) revealed that the larger mEPSCs occurring when frequency

has returned to baseline levels have faster rise time as compared to control. Also, in some cells, distribution histograms of mEPSC amplitude clearly showed the presence of multiple equidistant peaks following stimulation, which could indicate multiquantal transmitter release from the presynaptic terminal.

In conclusion, this investigation illustrates the presence of two concomitant forms of synaptic plasticity arising from a HFS delivered to the excitatory synapses of the SON; one for amplitude and one for frequency of mEPSCs. Both of these forms arise from the presynaptic terminal. This result shows the capacity for sophisticated modulation of incoming excitatory information to the SON. Further investigations into the mechanisms behind these two forms of plasticity will be useful in clarifying the ways in which the excitatory afferents to the SON can modify the activity of the MCNs.

Acknowledgments

I would like to thank my supervisor Dr. Michiru Hirasawa for being an extraordinary mentor, a true scientist, and a great role model.

I would also like to thank Christian Alberto for bestowing unto me some of his stellar organizational skills and for all of his help during my master's project.

I would also like to thank my fellow lab mate, Matthew Parsons, for his stimulating conversation, great mathematical skills, and constant intellectual support.

I would also like to thank my supervisory committee members, Dr. Carolyn Harley and Dr. Penny Moody-Corbett, for their animated and encouraging dialogue.

Lastly, I would like to thank CIHR for providing the funding for my work as a master's student.

Table of Contents

List of Figures

List of Abbreviations (in alphabetical order)

aCSF: artificial cerebrospinal fluid

ACTH: adrenocorticotropic hormone

ampSTP: short-term potentiation of the amplitude of mEPSCs

ANP: atrial natriuretic peptide

AVP: vasopressin

BNST: bed nucleus of the stria terminalis

CVO: circumventricular organ

DAP: depolarizing afterpotential

DNQX: 6,7-dinitroquinoxaline-2-3-dione

EPSP: excitatory postsynaptic potential

extended ampSTP: extended amplitude potentiation

extended freqSTP: extended frequency potentiation

freqSTP: short-term potentiation of the frequency of mEPSCs

GFAP: glial fibrillary acidic protein

HFS: High frequency stimulation

IR-DIC: Infrared differential interference contrast

LTP: long-term potentiation

MCN: magnocellular neuron

mEPSC: miniature excitatory postsynaptic current

NAcc: nucleus accumbens

NTS: nucleus tractus solitarius

OT: oxytocin

OVLT: organum vasculosum of the lamina terminalis

PVN: paraventricular nucleus

SCN: suprachiasmatic nucleus

SFO: subfornical organ

SON: supraoptic nucleus

STP: short-term potentiation

TTX: tetrodotoxin

CHAPTER 1

INTRODUCTION

1.1: Oxytocin and Vasopressin Background

1.1.1: General

The neuroendocrine system is a very diverse entity, containing several hormones that exert widespread actions in the periphery. Two of the most prominent of these hormones are oxytocin (OT) and vasopressin (AVP). The chemical structures of these two nonapeptides were discovered in the 1950's by the American biochemist, Vincent Du Vigneaud. These neuropeptides are synthesized predominantly in cell bodies of the magnocellular neurons (MCN) of two hypothalamic nuclei: the supraoptic nucleus (SON) and paraventricular nucleus (PVN). Synthesis also occurs to a lesser extent in the parvocellular neurons of the PVN, suprachiasmatic nuclei (SCN), bed nucleus of the stria terminalis (BNST) and the medial amygdala (Sofroniew, 1983).

MCNs of the SON and PVN send their axon terminals to the posterior pituitary via the hypothalamoneurohypophysial tract where, upon appropriate stimulation, such as an increase in plasma osmolality, OT and AVP are released directly into the bloodstream. This expulsion of hormone into the periphery is a process known to be immediately coupled to the electrical activity of MCNs (Poulain and Wakerly, 1982; Renaud and Bourque, 1991).

Traditionally it was thought that the main endocrine functions of OT were related to parturition and lactation, while AVP functioned in the facilitation of water absorption by the kidney and the contraction of arterial smooth muscle, which are very important in cardiovascular regulation. But the fact that OT is found in the posterior pituitary and the plasma in both males and females strongly suggests that OT has further physiological functions (Gimpl and Fahrenholz, 2001). Furthermore, the presence of functional OT and AVP receptors in many areas of the body indicate that there are likely many physiological actions in which these neuropeptides participate.

1.1.2: Subtypes of Oxytocin and Vasopressin Receptors

OT- and AVP-receptors are both classified as G-protein coupled receptors. AVP action has been found to be mediated by three different subtypes of AVP-receptors, namely, V1a, V1b, and V2. These are all located in discrete areas of the body, exerting varying physiological actions both peripherally and centrally (Lolait et al., 1992; Morel et al., 1992; Thibonnier et al., 1994). The activation of the V1 receptors results in the activation of Gq/G11 or $G_{i/o}$ proteins, while the activation of V2 receptors involves activation of the Gs protein and protein kinase A (Barberis et al., 1998; Valenti et al., 2005). Unlike AVP, only one OT receptor subtype has been characterized, and this has been found both centrally and peripherally (Adan et al., 1995). This was demonstrated by Gimpl and Fahrenholz (2001) with the discovery that there existed only one OT-receptor gene in mice. High concentrations of OT can interact with all three types of AVP receptors (Thibonnier et al., 1999), and likewise, AVP can also bind to the OT

receptor, with an almost equal affinity to that of OT itself (Gimpl and Fahrenholz, 2001). OT receptors, which are widely expressed both centrally and peripherally (Gimpl and Fahrenholz, 2001), are functionally coupled to G_q proteins like the V1 receptors, which upon activation, cause a cascade of events leading to the formation of inositol trisphosphate which triggers the release of Ca^{2+} from intracellular stores (Gimpl and Fahrenholz, 2001).

1.1.3: Function and Localization of Oxytocin and Vasopressin Receptors

The action of AVP is most closely associated with osmolality. Activation of the V2-receptors located in the kidney mediate the main physiological effect of AVP; the antidiuretic action (Lolait SJ et al., 1995; Thibonnier M et al., 1994; Knepper, 1997). V2-receptor expression in the kidney is quite dense and widespread, encompassing the thick ascending limbs as well as the medullary collecting duct cells (Nonoguchi H et al., 1995; Nielsen S et al., 1995). Specifically, activation of the V2 receptors results in the increased permeability of the renal collecting ducts to water, facilitating reabsorption of water from the urine, back to the bloodstream (Yamamoto et al., 1995).

The V1a receptor is expressed in smooth muscle, the liver, and the brain. V1a receptor activation in smooth muscle (particularly vascular smooth muscle but also myometrium smooth muscle), has direct effects on blood pressure by helping to maintain vascular tone as well as stimulate contraction (Nemenoff, 1998). In addition to smooth muscle, V1a receptors are also expressed in the liver where activation by AVP regulates many metabolic functions, particularly those involved in glucose homeostasis (Aoyagi, et

al., 2007). Like V1a receptors, V1b receptors are also located centrally where they mediate stress responses in the limbic system (Griebel et al., 2002). They are also expressed in the anterior portion of the pituitary gland where activation of these receptors regulates the secretion of the pituitary hormone adrenocorticotrophin (ACTH), an important signaling molecule in the hypothalamic-pituitary-adrenal axis (Antoni, 1993).

The V1a receptor is widely expressed in the brain at high density in limbic areas such as the septum, the amygdala, the BNST, and the nucleus accumbens (NAcc). They are also found in the SON itself, SCN, dorsal tuberal region of the hypothalamus, and nucleus tractus solitarius (NTS) as well as the spinal cord, suggesting V1a is the main receptor responsible for central actions of AVP (Tribollet et al., 1988).

The action of OT is most closely associated with female reproduction, where it has been shown that OT receptor density increases in the uterus throughout the course of pregnancy (Shojo and Kaneko, 2000; Verbalis, 1999). OT in the bloodstream is known to cause contraction of both endometrium smooth muscle during labour and of the myoepithelial cells that surround the alveoli of the mammary gland to elicit milk ejection in response to suckling (Blanks and Thornton, 2003; Kiss and Mikkelsen, 2005). While these are its classical physiological functions, the OT-receptor is widespread throughout the body and is found not only in the uterus and mammary glands, but also the brain, kidney, thymus, ovary, heart, and blood vessels (Shojo and Kaneko, 2000; Gimpl and Fahrenholz, 2001; Gould and Zingg, 2003).

OT receptors in the kidney, heart and vasculature, like AVP receptors, make a significant physiological contribution to two intricately connected systems; the renal and the cardiovascular systems. In the cardiovascular system, OT-receptor activation acts

directly, causing relaxation of vascular smooth muscle, a reduction in heart rate, and a decrease in the force of contraction (Gutkowska et al., 2000; Favaretto et al., 1997). OT also stimulates the release of atrial natriuretic peptide (ANP) from the heart, which has a major impact on hydromineral homeostasis, and as a consequence, cardiovascular function (Gutkowska et al., 2000). Furthermore, Jirikowski et al. (1986) determined that ANP is coexpressed in hypothalamic OT neurons, which not only suggests that OT stimulates the release of ANP, but that it may be concomitantly released from the posterior pituitary into circulation.

1.1.4 Oxytocin and Vasopressin and Osmotic Homeostasis

The role of OT in controlling hydromineral homeostasis is almost as important as that of AVP, with Conrad et al. (1986) demonstrating that OT was efficacious as a natriuretic agent, even in the absence of AVP. Furthermore, it appears that hyperosmotic stimulation increases both the expression of AVP mRNA and the transcription of the OT gene in the SON and PVN (Meister, et al., 1990; Lightman and Young, 1987; Burbach et al., 1984). Similarly, hyperosmotic and hypovolemic stimuli both induce the release of OT and AVP from MCNs triggering these peripheral effects (Share, 1988; Gimpl and Fahrenholz, 2001). As it stands, both types of hypothalamic MCNs release large amounts of stored OT and AVP into the bloodstream in response to physiological deviation in water balance and this is accomplished by a functional remodeling of neuronal activity (Kiss and Mikkelsen, 2005). Electrical activity of MCNs is enhanced or diminished respectively during periods of increased or decreased plasma osmolality (Brimble and

Dyball, 1977), and not surprisingly, circulating concentrations of both OT and AVP vary depending on plasma osmolality (Stricker and Verbalis, 1986). This is supported by evidence from Miyata et al. (1994) who showed that either sustained or chronic injection of hypertonic saline or water deprivation caused a transient increase in c-FOS expression in hypothalamic MCNs which was reversible within 24 hours of rehydration.

1.1.5 Oxytocin, Vasopressin and Behaviour

Recently, research pertaining to central AVP- and OT-receptor mediated function has been accumulating. The omnipresence of OT and AVP receptors throughout the brain serves as a testament to their central roles (Raggenbass, 2001). Though synthesis of these neuropeptides occurs centrally at sites outside of the neurohypophysial system, MCNs of the SON and PVN also release neuropeptide dendritically, and this is a significant source of central OT and AVP (Landgraf and Neumann, 2004). The behaviours that these neuropeptides support as a consequence of their central actions are quite different from one another in contrast to the parallel effects seen peripherally. For example, in the limbic system, particularly the amygdala, a key area in the processing of emotion and stress responses, OT and AVP appear to have opposite effects on behavior. AVP appears to augment aggressive behaviors, stress responses, and anxiety levels (Ebner et al., 2002; Griebel et al., 2002; Bielsky, et al., 2004) while OT has been shown to attenuate stress and anxiety while enhancing maternal bond formation and social behaviors (Uvnas-Moberg, 1998; Gimpl and Fahrenholz, 2001; Windle et al., 1997; Febo et al, 2005).

1.2: Activation of MCNs

1.2.1: Glutamate Receptors in the SON

Glutamate binds to both ionotropic (NMDA and AMPA/kainate) and metabotropic glutamate receptors which exist on the MCNs (Stern et al., 1999; Schrader and Tasker, 1997). Application of the broad spectrum glutamate antagonist kynurenic acid largely attenuates and often eliminates evoked EPSPs and spike trains in the MCNs of the SON (Gribkoff and Dudek, 1990).

In the SON, there are a larger number of AMPA/kainate-type glutamate receptors, as compared to NMDA-type, which mediate the spontaneous as well as the evoked excitatory postsynaptic potentials (Meeker et al. 1994; Wuarin and Dudek, 1993; Gribkoff and Dudek, 1990). At resting potential, it was shown that glutamate was responsible for all of the spontaneous EPSCs in MCNs, and that this type of fast excitatory transmission was primarily a consequence of AMPA/kainate receptor activation (Wuarin and Dudek, 1993; Edmonds et al. 1995), though work by Hatton et al. (2002) suggests some role of cholinergic transmission as well, though this has been shown to desensitize with repetitive stimulation.

NMDA-receptor activation in MCNs of the SON appears to be associated with a cascade of responses. In addition to sodium ions, NMDA-receptors are also permeable to other ions, notably calcium ions, which upon arrival into the intracellular milieu, can lead to long lasting changes in the neuron (Bliss and Collingridge, 1993).

1.2.2: Glutamate Projections to the SON

Approximately 20% of the synaptic inputs to the SON are glutamatergic and these are distributed evenly over the OT and the AVP neurons (Meeker et al. 1993; El Majdoubi et al. 1996). These glutamatergic projections arise from a number of intra- and extrahypothalamic brain areas. Retrograde labeling combined with autoradiography revealed that these projections come from several telencephalic regions such as the amygdala, BNST, the septum and the preoptic area, but are more numerous from the diencephalic regions such as the SON itself and its perinuclear regions, the PVN, SCN, as well as the hypothalamic ventromedial, paraventricular, and dorsomedial nuclei, the ventral thalamus, and premammillary and supramammillary nuclei (Csaki, et al., 2002). Electrophysiological and anatomical data suggest that some of the afferent inputs to the SON come from adjacent hypothalamic areas (Boudaba et al., 1997; Roland and Sawchenko, 1993). Interestingly, the MCNs of the PVN and SON have been shown to be intricately connected by glutamatergic synaptic circuits, both ipsilaterally via a PVN-SON connection, as well as contralaterally via a PVN-PVN connection (Boudaba and Tasker, 2006). This is anatomically suggestive of a capability of MCNs to coordinate bursts between nuclei, resulting in synchronization upon activation.

One brain area with prominent, direct glutamatergic projections to the SON is the organum vasculosum of the lamina terminalis (OVLT), which sits in the anteroventral third ventricle wall. The OVLT is one of several circumventricular organs (CVO). CVOs are located in close proximity to the ventricular system and along with the OVLT, also include the posterior pituitary, subfornical organ (SFO), area postrema, choroid

plexus, the median eminence, pineal gland, and subcommissural organ. These areas lack a blood brain barrier and therefore are believed to function in the detection of changes in the concentration of various circulating compounds. The OVLT and SFO contain osmoreceptors which are responsive to changes in ionic concentrations of the plasma and to hormones such as ANP and angiotensin II (Johnson and Gross, 1993; McKinley et al., 1999). OVLT neurons are activated by an increase in plasma osmolality and have a characteristic low threshold spike which acts as the driving potential for the generation of brief bursts of action potentials with firing frequencies ranging between 50 and 80 Hz. (Nissen, et al., 1993). Along with several other brain areas such as the median preoptic area, anterior lateral hypothalamus, SFO, anteroventral region of the third ventricle (AV3V), SON, PVN, habenula, stria medullaris, and the medial septal area, the OVLT acts as part of an integrative neural network functioning in the maintenance of proper water and electrolyte balance (Bourque and Oliet, 1997).

1.2.3: Glutamate and MCN activity

MCNs of the SON display an intermittent bursting or phasic activity to optimize the release of OT or AVP from their axon terminals. These characteristic firing patterns depend on the intrinsic regenerative properties of MCNs (Andrew and Dudek, 1983; Armstrong et al., 1994) and extrinsic factors (Hu and Bourque, 1992; Jourdain, et al., 1998; Bourque, et al., 1998; Ludwig and Pittman, 2003; Li, et al., 2007). Research strongly suggests that glutamate is one of the main neurotransmitters involved in the

regulation of OT and AVP release from the MCNs (Costa et al. 1992; Bisset & Fairhall 1996; Sladek et al. 1998).

Glutamate is the major excitatory neurotransmitter in the SON and is known to be essential for the onset and maintenance of bursting activity of MCNs, both *in vivo* and *in vitro* (Wakerly and Noble, 1983; Hu and Bourque, 1992; Nissen et al., 1995; Jourdain et al., 1998; Brown et al., 2004). Increasing levels of frequency and fluctuation of basal firing between bursts are driven by excitatory synaptic inputs and promote bursting activity in OT neurons (Israel et al., 2003; Moos et al., 2004), with clusters of EPSPs underlying bursts (Dudek and Gribkoff, 1987; Jourdain et al., 1998). Furthermore, synchronization of action potential firing between a pair of OT neurons relies on excitatory transmission (Israel et al., 2003). Bursting of MCNs also depends on local neuropeptide release from the dendrites of these neurons (Lambert et al., 1993; Jourdain et al., 1998). Glutamate can initiate this mechanism by inducing dendritic peptide release through the activation of NMDA receptors (de Kock, et al., 2004). Once dendritic release is triggered, neuropeptides may amplify themselves in a positive feedback manner stimulating further dendritic release (Moos et al., 1984; Ludwig et al., 2005). Interestingly, Hirasawa et al. (2003) found AVP inhibited AMPA-induced currents in AVP neurons through V1a receptors, while it facilitated these same currents in OT neurons via OT receptors. This is supported by work which also links dendritic release to the activation of dendritic autoreceptors (Richard et al., 1991). Furthermore, glutamate seems to be involved in OT-induced morphological remodeling in the SON (Langle et al., 2003). Such structural plasticity is known to occur *in vivo* during periods of high hormone demand such as lactation and dehydration (Hatton, 1997).

1.3: The Intrinsic Properties of MCNs

1.3.1: AVP Neurons and Phasic Firing

Thus far it is clear that there are numerous similarities between the two subtypes of neuroendocrine cells of the hypothalamoneurohypophysial system. OT and AVP are similar in terms of structure and receptor subtypes and have many similar target tissues for action. However, they differ in terms of their firing patterns (Poulain and Wakerly, 1982). AVP neurons respond to increases in plasma osmolality, decreases in blood volume, and changes in blood pressure by a phasic burst firing pattern (Brimble and Dyball, 1977; Armstrong et al., 1995). During phasic firing, individual AVP neurons alternate between periods of activity and quiescence. The active periods typically have firing frequencies between 5-15 Hz, last about 30 seconds, and are separated by intervals of relative quiescence, with a firing frequency of less than 1 Hz (Renaud and Bourque, 1991). An active phase can be initiated by glutamate application, and be sustained long after the glutamate stimulation has ended (Wakerly and Noble, 1983), suggesting that these cells also have intrinsic properties which are responsible for the persistence of their burst firing patterns. Andrew and Dudek (1983) found that in phasic MCNs, a single action potential was followed by a slow depolarizing afterpotential (DAP) and found that in periods of repetitive firing, these DAPs could summate to form slower, persistent depolarizations termed plateau potentials. The plateau potentials appear to underlie the burst firing pattern seen in these neurons (Andrew and Dudek, 1983, 1984).

1.3.2: OT Neuron Bursting

In contrast to AVP neurons, OT neurons are characterized by shorter, but more robust, burst firing patterns which occur during lactation. These bursts range between 50-80 Hz, last about 1-4 seconds and are synchronized among OT neurons (Poulain and Wakerly, 1982; Belin et al., 1984), resulting in volleys of OT released into the bloodstream. This synchronization is thought to arise partially from concomitant dendritic release of OT, activating dendritic OT receptors and thus further enhancing excitation (Ludwig, 1998). Wang and Hatton (2007) induced burst firing in OT neurons with exogenous OT application; an effect which was blocked with administration of an OT receptor antagonist. During suckling these bursts are typically separated by 5-20 minute intervals and thus, take on a pattern of pulsatile OT release, with each burst immediately preceding each milk ejection (Belin et al., 1984; Armstrong and Hatton, 2006). This release pattern could have numerous advantages such as circumventing OT receptor desensitization at the myoepithelial cell, allowing for a maximal contraction, as well as giving the OT neurons themselves a chance to recover from release fatigue (Bickness, 1988), since this is a highly energy-dependent process. It is likely that these firing patterns are triggered by glutamate since application of ionotropic glutamate receptor blockers block the burst generation seen in OT neurons (Wang and Hatton, 2007).

1.3.3: Shared Intrinsic Properties of AVP and OT Neurons

Though their patterns of firing are quite distinct, OT and AVP neurons share many similar intrinsic membrane properties. Measurements conducted by Armstrong et al. (1994) revealed that there were no discrepancies between OT and AVP neurons in their resting membrane potential, input resistance, membrane time constant, action potential characteristics, or spike hyperpolarizing after-potential (Armstrong, et al., 1994). The resting membrane potential for MCNs is around -65 mV (Armstrong et al., 1994). Magnocellular neurons are known for their relatively high input resistance in comparison to other neuronal populations. In the experimental protocol used here, employing the nystatin perforated patch clamp recording technique, input resistances for OT and AVP neurons were approximately 1.013 GΩ ± 0.53, similar to that recorded for MCNs of the PVN (Gordon and Bains, 2005). With such high input resistances, even very slight changes in neurotransmission onto MCNs could have a very large impact on their excitability, as seen with the effects of spontaneous glutamatergic transmission to the SON, which in calcium free medium was capable of generating action potentials (Inenaga et al., 1998).

MCNs also exhibit a transient outward current (Armstrong, et al., 1994; Nagatomo, et al., 1995) which results in a longer latency to first spike, which we used to identify MCNs in addition to their anatomical features (Figure 1a). This transient outward current results from the activation of A-type potassium channels (Shibata, et al., 2000). These channels are activated upon depolarization from hyperpolarized potentials, hence resisting further depolarization. Therefore, neurons expressing A-currents take longer to

reach the threshold for action potential firing. This is in fact a graded response, meaning that the more hyperpolarized the initial membrane potential of the neuron, the longer the latency to threshold (Shibata, et al., 2000).

1.4: Plasticity in the SON

1.4.1: Structural Plasticity in the SON

The SON has been shown to undergo very prominent morphological synaptic reorganization in response to conditions that result in increased peripheral hormone demand. During pregnancy and lactation it was shown that the astrocytic processes that usually surround the MCNs were withdrawn. This is known as glial retraction, and it increases direct soma to soma contact between MCNs, the number of synaptic contacts, and gap-junction formation between OT neurons (Andrew et al. 1981; Micevych et al. 1996; Hatton et al. 1987). Specifically, the number of glutamatergic synapses afferent to the SON increases during lactation, with similar structural plasticity also seen in periods of dehydration (El Majdoubi et al., 1997, Hawrylak et al., 1998). Hawrylak et al. (1998) found that dehydration resulted in a significant reversible reduction in immunoreactivity to fibrillary acidic protein (GFAP; a marker for astrocytes) in the SON of rats. This was interpreted as a reflection of glial retraction, which would enhance direct soma to soma contact between magnocellular neurons.

1.4.2: Structural Plasticity and Dendritic Release

MCNs of the SON have been shown to release neuropeptide from their dendrites in response to activation of NMDA receptors (Ludwig, 1998; Ludwig et al., 2005; de Kock et al. 2004). It is this dendritic release of neuropeptide in addition to glutamate which has

been suggested to be the trigger for the prominent morphological changes which occur in this nucleus (Theodosis et al., 2006). Dendritic release of neuropeptide was also shown to occur in response to high frequency stimulation delivered to excitatory afferents when the stimulation was delivered in current clamp mode; a situation which allows NMDA-receptor activation (Kombian et al., 1997).

Exogenous OT application mimicked the glial retraction seen during parturition, lactation, and dehydrated states in a manner which depended on both glutamate receptors and OT receptors and was also shown to be reversible upon washout (Langle et al., 2003). During lactation, it was also found that GABAergic transmission was decreased as a consequence of increased somatodendritic release of OT (de Kock et al., 2003; 2004). It has been shown that dendritic OT release (and likely dendritic AVP release as well, though the data are less conclusive) can also inhibit glutamatergic transmission by activating dendritic autoreceptors which trigger the release of endocannabinoids, which in turn, act retrogradely on endocannabinoid receptors located at the presynaptic terminal (Kombian et al., 1997, Hirasawa et al., 2004, Kombian et al., 2002). This OT induced inhibition targets evoked excitatory transmission through modulation of presynaptic calcium channels (Hirasawa et al., 2001). Furthermore, the retraction of glial processes is also associated with a reduction in glutamate clearance, which results in inhibition of glutamatergic transmission at the presynaptic terminal due to activation of presynaptic metabotropic glutamate receptors (Oliet et al, 2001).

1.4.3: Synaptic Plasticity: LTP of Evoked EPSCs

Afferents to the SON are also targets for activity dependent synaptic plasticity observed by electrophysiological means. Panatier et al. (2006) revealed that long-term potentiation (LTP) of the amplitude of AMPA-receptor mediated evoked EPSCs occurs following high frequency stimulation (HFS) to afferent fibers. Their observations were likely due to changes occurring at the postsynaptic neuron since LTP was blocked by chelating postsynaptic calcium or by bath application of an NMDA-receptor antagonist, and were not associated with a change in the probability of neurotransmitter release from the presynaptic terminal.

1.4.4: Synaptic Plasticity: Short-term Potentiation of Miniature EPSCs

A train of stimulation to excitatory afferents innervating the SON induces a long barrage of spontaneous EPSP/EPSCs leading to a slow depolarization and afterdischarge of the postsynaptic MCNs that continues after the stimulation has ended, for many seconds to many minutes depending on the frequency and pulse number of the stimuli (Hatton et al., 1983; Dudek and Gribkoff, 1987; Kombian et al, 2000). Work by Kombian, et al. (2000) revealed that a HFS to the excitatory afferents to the SON induced a robust increase in the frequency and amplitude of AMPA receptor-mediated spontaneous EPSCs which lasted for 5 to 20 minutes. These EPSCs are TTX-insensitive, and are therefore equivalent to miniature EPSCs. In contrast, the induction of such an increase is TTX sensitive, suggesting that action potential firing of the excitatory

afferents is necessary. This response is unique due to its time course in that it is substantially longer than synaptic facilitation (which lasts for less than half a second and is quite common in CNS synapses), but much shorter than LTP, which can last for several hours *in vitro* (Xu-Friedman and Regehr, 2004, Lynch, 2004). Based on the duration of the response to stimulation, this phenomenon was called short term potentiation (STP).

STP of the frequency of mEPSCs (referred to as freqSTP in this thesis) is composed of two phases, the first of which has a large magnitude and fast decay, and the second of which decays much more gradually (Quinlan et al., 2008). FreqSTP relies on voltage-gated calcium channels for initiation, and the sequestration of calcium into, and subsequent release from, the mitochondria for maintenance (Quinlan et al., 2008). FreqSTP can be induced multiple times at the same synapse, and is inhibited by GABA through activation of presynaptic $GABA_B$ receptors, reducing both the magnitude and the duration of STP (Kombian et al., 2000; Kombian et al., 2001). This is an indication that freqSTP is a presynaptic phenomenon. Furthermore, freqSTP does not involve the activation of postsynaptic NMDA-receptors or the neuropeptides OT and AVP, which can be released from the postsynaptic cell and act as retrograde messengers (Kombian et al., 2000). Thus, both the induction and manifestation of freqSTP seem to be presynaptic.

In contrast, less is known about the nature of the potentiation of mEPSC amplitude in response to HFS. Large mEPSCs have been shown to appear immediately after HFS, and the amplitude of these events displays a skewed distribution with the presence of multiple peaks (Kombian et al., 2000). These peaks were equidistant from the first peak and

appeared to conform to a Gaussian distribution. The number of peaks increased with HFS, indicative of multiquantal transmitter release (Kombian et al., 2000). The time course and mechanism of such changes remains unknown.

STP is suggested to have a physiological role as it is tightly coupled to an increase in action potential firing of the MCNs, further supporting findings from Inenaga et al. (1998) that mEPSCs can influence the excitability of the MCNs (Kombian et al., 2000). Similar results were also found in the PVN when it was shown that brief stimulation to the glutamatergic afferents was associated with a period of asynchronously released quanta which contributed to a prolonged period of postsynaptic spike activity in the MCNs (Iremonger and Bains, 2007). Therefore it is plausible that any enhancement or weakening of this phenomenon could have a significant impact on the excitability of MCNs and as a consequence, influence the release of hormone to the periphery. Furthermore, STP was shown to be a graded response, increasing in magnitude as stimulation frequencies increased up to 100 Hz, a frequency range close to that from the OVLT projection to the SON. OVLT neurons are activated by an increase in plasma osmolality and have a characteristic low threshold spike which acts as the driving potential for the generation of brief bursts of action potentials with firing frequencies ranging between 50 Hz to 80 Hz (Nissen, et al., 1993). Given that even a short train of action potentials (10 pulses) is sufficient to induce STP, it is likely that this phenomenon observed *in vitro* also takes place *in vivo* and plays a physiological role.

1.5: Aims and Hypotheses

The goal of the present work was to better understand the short term potentiation in response of mEPSCs to HFS, particularly the amplitude component. It is known that the amplitude of mEPSCs increases immediately after stimulation, but as yet it is unclear at to whether this is a by-product of the freqSTP or if it is its own distinct form of synaptic plasticity. Therefore, a deeper understanding of the mechanism behind the potentiation of mEPSC amplitude was sought. This thesis project had the following three aims.

Aim 1: To characterize the time course of the mEPSC amplitude response and to determine whether its time course can be differentiated from that of freqSTP.

Aim 2: To investigate the source of variation in the magnitude of STP among MCNs. Here it was hypothesized that variation in responses might be accounted for by the basal synaptic activity, the phenotype of the postsynaptic neuron, be it an OT or an AVP neuron, or the strength of the stimulation protocol employed.

Aim 3: To examine the time course of the mEPSCs and determine whether HFS alters characteristics of mEPSCs other than their frequency and amplitude.

CHAPTER 2

METHODS

All experiments were carried out in accordance with guidelines established by the Canadian Council on Animal Care and were approved by the Memorial University Internal Animal Care Committee. An effort was made to use only the necessary number of animals required to yield reliable results.

2.1: Slice Preparation:

Male Sprague-Dawley rats (60-100 g) were deeply anesthetized using halothane prior to decapitation. The brain was rapidly removed and 250 μm thick coronal sections containing the SON were generated in a 0-2°C buffer solution composed of the following (in mM): 87 NaCl, 2.5 KCl, 1.25 NaH_2PO_4, $7MgCl_2$, 0.5 $CaCl_2$, 25 $NaHCO_3$, 25 glucose, 30 sucrose, 3 pyruvic acid, and 1 ascorbic acid, bubbled with 95% O_2, 5% CO_2 gas. Slices were incubated at 33-34°C for 45 minutes and then at room temperature until recording in bubbled artificial cerebrospinal fluid (aCSF) composed of the following (in mM): 126 NaCl, 2.5 KCl, 1.2 NaH_2PO_4, 1.2 $MgCl_2$, 2 $CaCl_2$, 25 $NaHCO_3$, 10 glucose, 1 ascorbic acid.

2.2: Electrophysiological Recording:

Slices were hemisected, placed into a recording chamber and perfused at 1.5-2.5 mL/min with aCSF at 33-34°C. Whole cell patch clamp recordings were done in the SON with a MultiClamp 700B amplifier (Molecular Devices, Sunnyvale, CA). Nystatin was used as a perforating agent to obtain access unless stated otherwise, where conventional whole-cell access was used. For nystatin perforated patch recording, the internal solution contained the following (in mM): 120 K-gluconate, 5 $MgCl_2$, 8 KCl, 10 EGTA, 40 HEPES, 4 Na_2-ATP, 0.3 Na-GTP, pH 7.3. Nystatin was dissolved in dimethyl sulfoxide (DMSO) with Pluronic F127 and added to the internal solution to yield a final concentration of 450 μg/mL. Glass electrodes had a tip resistance of 2-7 MΩ when filled with the internal recording solution. Series/access resistance of 10-40 MΩ was normally attained within 20 minutes after formation of a gigaohm (1-8 GΩ) seal. For conventional whole cell recording, internal solution consisted of (in mM): 123 K-gluconate, 2 $MgCl_2$, 8 KCl, 0.2 ethylene glycol-bis(b-aminoethyl ether)-N,N,N9,N9-tetraacetic acid (EGTA), 10 N-2-hydroxyethylpiperazine-N9-2-ethanesulfonic acid (HEPES), 4 Na_2-ATP, 0.3 Na-GTP, pH 7.3. EGTA was increased to 10 mM when necessary.

Infrared differential interference contrast optics (IR-DIC; DM LFSA, Leica Microsystems) were used to visualize the SON in the hemisected slice of tissue. Experiments were conducted in voltage-clamp mode at a holding potential of -80 mV in the presence of picrotoxin (50 μM) to isolate EPSCs. Input resistance (R_{input}) and

access resistance (R_a) of all cells were monitored every minute by applying a 20 mV hyperpolarizing pulse for 100 msec. Cells that showed 15% or greater change in these parameters were not included in the data analysis.

Bipolar tungsten-stimulating electrodes were placed dorsal to the SON in order to evoke synaptic responses and to apply HFS (one of either 50 pulses at 50 Hz, or 2 sets of 100 pulses at 100 Hz, separated by a 10 second interval). It is unlikely that either stimulation protocol would have caused any extraneous excitatory input that could have compromised the integrity of the postsynaptic cell. It has previously been demonstrated that MCNs of the SON have a strong resistance to glutamate toxicity (Hu et al., 1992). All cells had a graded evoked synaptic response to increasing stimulus intensity. The response giving 50-70% of the maximum evoked EPSC was used to apply HFS.

Both evoked EPSCs and spontaneous EPSCs (sEPSC) were completely blocked by 6,7-dinitroquinoxaline-2-3-dione (DNQX; 10 μM), indicating that they were non-NMDA receptor mediated. Previously reported experiments illustrated that while the evoked EPSCs are abolished by tetrodotoxin (TTX; 1mM), the sEPSCs are TTX-resistant (Kabashima et al., 1997, Boudaba et al., 1997, Schrader and Tasker, 1997, Kombian et al., 2000). This may be due to the nature of the coronal slice preparation in those experiments in that the soma of the afferent neurons to the SON are severed, therefore preventing any generation of action potential firing that would propagate down to the presynaptic terminal. In contrast, sEPSCs recorded in this preparation were equivalent to miniature EPSCs (mEPSC). In this study all recordings were done without TTX because STP induction is dependent on high frequency action potential firing of the presynaptic fibers (Kombian et al., 2000). All data were collected using pClamp 9 software

(Molecular Devices, Sunnyvale, CA). Membrane currents were acquired at a 2-10 KHz sampling rate, filtered at 1 KHz, and stored for offline analysis.

2.3: Data Analysis:

Miniature EPSCs (mEPSCs) were detected visually using Mini Analysis 6.0 software (Synaptosoft, Decatur, GA). mEPSCs clearly standing out from the background noise were selected based on shape, those demonstrating a fast (1-2 msec rise) and an exponential decay (5-10 msec) being the prototype for consideration. In the case of amplitude analysis for mEPSCs, only those currents showing a clearly defined baseline and peak with a smooth rise slope were used. Any events showing overlap with other events were not used if the baseline to peak was not clear. In all cells, at least the first 8 minutes following recording were analyzed, and whenever possible, more. In cases where a pharmacological manipulation was carried out and a change in input resistance occurred or a change in membrane potential arose, analysis was truncated. Evoked EPSCs were measured using Clampfit 9.2 (Molecular Devices, Sunnyvale, CA). Statistical comparisons were performed by using appropriate tests, i.e. Kolmogorov-Smirnov test for individual cells, two-way repeated measures ANOVA for multi-factor paired group data, two-way ANOVA for multi-factor unpaired group comparisons, and unpaired or paired Student's *t* tests for group comparisons as appropriate. A value of $p < 0.05$ was considered significant.

Time-effect plot of the frequency of mEPSCs obtained from individual cells were fitted with one or two-exponential curves using Prism 4 (GraphPad Software Inc.). The half-life of each exponential component was also calculated using the software.

Following stimulation, amplitude and frequency were considered back to baseline once they fulfilled two criteria: there had to be three consecutive minutes during which the amplitude and/or the frequency were between 90-110% of baseline using normalized data, and also, statistical analysis using the Kolmogorov-Smirnov test had to no longer be statistically significant in that same series of three minutes.

2.4: Drugs:

All drugs were bath-perfused (with the exception of EGTA) at final concentrations by dissolving aliquots of stock in aCSF. The solvents were diluted at least by 1000 times. All compounds were purchased from Sigma-Aldrich (St. Louis, MO), except DNQX, D(-)-2-amino-5-phosphonopentanoic acid (D-APV) both from Tocris Bioscience (Ellisville, MO), EGTA from OmniPur, and Pluronic F127 from BASF.

CHAPTER 3

RESULTS

3.1: MCN Identification and Response to HFS

Whole-cell patch clamp recordings were performed in 38 magnocellular neurons (MCNs) of the SON. Putative MCNs were initially identified by their large size, tight juxtaposition to one another, and location immediately lateral to the optic chiasm. Electrophysiologically, all MCNs were identified based on the characteristic delayed onset to action potential generation in response to a depolarizing current injection (Fig. 1A; Tasker and Dudek, 1991; Armstrong, 1995). Putative OT neurons were identified by the presence of both an inward rectification as well as a sustained outward rectification to a series of hyperpolarizing steps from more depolarized potentials (200 msec steps starting at -40 mV down to -130 mV in 10 mV increments; Fig. 1B), while AVP neurons were classified by an absence of rectification, displaying a linear current-voltage relationship to the same protocol (Fig. 1C; Stern and Armstrong, 1995, Hirasawa et al., 2003).

Two stimulation protocols to excitatory afferents were effectively employed in this study (50 Hz, once for 1 s; 100 Hz, twice for 1 s), and both reliably generated STP. In all of the cells tested, a robust increase in the frequency and the amplitude of mEPSCs typically lasting between 3 and 20 minutes was observed (Fig. 2A). While the initial magnitude and duration of potentiation varied among cells, within a given cell, mEPSC-

STP was reversible and reliably reproduced by repeated application of HFS as shown previously (Kombian, et al., 2000; data not shown). The number and size of mEPSCs were dramatically elevated immediately after HFS, a response which was still evident minutes later, as compared to control (Fig. 2B, C, and D). The recordings performed herein suggest that this is a property of the excitatory afferents for both AVP and OT neurons as previously reported (Kombian et al., 2000).

3.2: Frequency increase following HFS

Immediately following HFS, mEPSC frequency increased, reaching approximately 30- to 40-fold in the first minute, and typically returned to baseline within 20 minutes in a two phase exponential fashion (Quinlan, et al., 2008). No statistical differences between the 50 Hz and 100 Hz stimulation protocols were seen in the frequency response (Fig. 3A; n=10 and 11 for the 50 Hz and 100 Hz protocols, respectively). Although most cells show a smooth decay to baseline (13/21 control cells) (Fig. 3B), a significant proportion display a noticeable second peak in the frequency time-effect plot, defined as a resurgence in mEPSC frequency following an initial decay, within 3-5 minutes post HFS (8/21 control cells) (Fig. 3C).

Variation in the peak magnitude (1^{st} minute post-HFS) and duration of the STP may have stemmed from the intercellular variation in the baseline value of frequency since the measured value was normalized to the mean baseline in order to obtain the magnitude of changes. The basal mEPSC frequency for cells recorded was 1.34 Hz ± 0.81 (n=21) which rose to 36.29 Hz ± 18.86 (n=21) in the first minute following HFS. A linear

regression analysis was used to address whether or not the frequency of mEPSCs in the control period (baseline) was correlated with the percent change of frequency in the first minute following stimulation, as well as the duration of potentiation of mEPSC frequency. The frequency of mEPSCs during control was negatively related to the percent change during the first minute (Fig. 4A; $p < 0.01$; $r^2 = 0.3463$; $n = 21$) which in turn was positively related to how long the frequency potentiation persisted (Fig. 4B; $p < 0.02$; $r^2 = 0.2700$; $n = 21$) but no direct relationship was seen with the frequency of mEPSCs during control and the duration of the frequency potentiation (Fig. 4C; $r^2 = 0.01943$; $n = 21$).

3.3: Amplitude increase following HFS

The amplitude of mEPSCs following HFS also significantly increased at this synapse, although percentage effects are much smaller than the increases in frequency. The amplitude response is variable between cells but no significant differences are seen between the averaged responses from the 50 Hz and 100 Hz protocols in this parameter (Fig. 5A; $n = 10$ and 11 for the 50 Hz and 100 Hz protocols, respectively). Since 50 Hz and 100 Hz stimulation protocols induced a similar STP of frequency and amplitude, data obtained using these protocols were pooled for the rest of the study.

Following HFS, the average amplitude per minute of mEPSCs increased approximately 140% of control levels in the first minute. The basal mEPSC amplitude was 20.27 pA ± 5.3 which rose to 30.38 pA ± 7.1 ($n = 21$). It is clear that during the first few minutes following HFS the distribution histogram obtained from every cell analyzed

became more skewed to the right, indicating the presence of larger mEPSCs as compared to control (Fig. 5B-I and B-II). Upon visual inspection, 16 out of 21 cells clearly revealed the presence of multiple peaks that are roughly equal in distance from the first peak immediately following stimulation in amplitude distribution histograms (Fig. 5C-II), a response seen by Kombian et al. (2000) who determined that they were equidistant from the first peak and conformed to a Gaussian distribution.

As with frequency, the measured amplitude was normalized to the mean baseline value in each cell in order to obtain the magnitude of amplitude response during STP. Therefore, variation in the degree of response of mEPSC amplitude may also stem from the intercellular variation in the baseline value for amplitude. Linear regression analysis revealed that there was a negative correlation between the mean amplitude of events in the control period and the percent change during the first minute following HFS (Fig. 6A; $p < 0.01$; $r^2 = 0.3084$; $n = 21$). Also, the maximum amplitude response to HFS was related to how long the amplitude remained elevated (Fig. 6B; $p < 0.01$; $r^2 = 0.3281$; $n = 21$). However, there was no significant relationship between the mean amplitude of events in the control period and the duration of the amplitude response directly (Fig. 6C; $r^2 = 0.03068$; $n = 21$).

Thus, these analyses have shown that both the frequency and amplitude of mEPSCs in the control period were related to the magnitude of their increase in the first minute following HFS, which in turn was related to the durations of frequency and amplitude responses, respectively.

3.4: Comparison of mEPSC Frequency and Amplitude During STP

Amplitude and frequency increase after HFS (ampSTP and freqSTP, respectively), but it was unknown whether there was a relationship between the time course of these two forms of STP. Based on the somewhat differing magnitude of responses and large variability in both parameters between cells, it was hypothesized that the duration of freqSTP would be independent of the duration of ampSTP. To test this hypothesis, a linear regression analysis of the time it took mEPSC frequency to return to baseline versus the time it took mEPSC amplitude to return to baseline was performed. MCNs were only included in this analysis if both parameters had fully recovered by the end of recording. It was found that there was no significant relationship (Fig. 7A; $r^2 = 0.03263$; $n = 8$). Comparisons were also made between the magnitudes of each parameter (responses during the 1st min) to determine if the cells which had large frequency increases also had large amplitude increases and it was found that there was no relationship (Fig. 7B; $r^2 = 0.01031$; $n = 21$). Therefore, in response to HFS it appears that STP is characterized by two components; potentiation of mEPSC frequency and of mEPSC amplitude, both persisting for minutes after stimulation but with independent time courses and degrees of response.

3.5: Extended Amplitude and Frequency STP

In this investigation it was found that 8 out of 17 MCNs demonstrated an extended amplitude potentiation (extended ampSTP; a persistent amplitude increase which outlasts

the enhancement in frequency response) while 9 out of 17 MCNs demonstrate an extended frequency increase (extended freqSTP; a persistent frequency increase which outlasts the enhancement in amplitude response). In 4 cells, the duration of the mEPSC amplitude response and the duration of the mEPSC frequency response were unable to be determined because the recordings were terminated before either parameter had returned to baseline levels (Fig. 8A).

Dissociation of the mEPSC amplitude and frequency responses allowed an opportunity to investigate the mEPSC amplitude increase without any influence from the frequency increase. Group data for the extended ampSTP group showed an average baseline amplitude of 18.56 pA ± 5.83 (n = 8), an average immediate post HFS amplitude of 30.78 pA ± 6.05 (n = 8), and an average amplitude of 24.31 pA ± 6.33 at the time point where frequency has fully recovered (Fig. 8B; n = 8; one-way repeated measures ANOVA; $p<0.001$). Miniature EPSCs both immediately after stimulation as well as when frequency had returned to baseline (late post HFS) were larger than control (n = 8; $p < 0.01$ and $p < 0.01$, respectively; student paired t-test), while no difference was seen between mEPSCs immediately post HFS and late post HFS.

Figure 9 shows expanded traces from three time points in a recording of a cell that displays a dramatic increase in the size of mEPSCs that remained elevated after the frequency returned to baseline. Distribution histograms of mEPSC amplitude show that during control most mEPSCs were clustered around approximately 20 pA (Fig. 10B) but immediately after stimulation many larger EPSCs appeared with some as large as 100 pA (Fig. 10C). These large events persisted even 5 minutes after frequency had returned to

baseline (Fig. 10D). These histograms indicate that the relative distribution of individual mEPSC amplitude during extended ampSTP is similar to that of 1-3 min post-HFS.

3.6: Extended Frequency and Amplitude Responses Not Unique to Phenotype or Stimulation Protocol

Since approximately half of the cells demonstrated an extended freqSTP while the other half demonstrated an extended ampSTP, it was reasoned that it could be due to the neuronal phenotype of the postsynaptic cell. What was found was that out of three putative OT neurons in which the recovery to baseline levels was followed, two showed an extended freqSTP while one showed an extended ampSTP (Fig. 11A). Out of seven putative AVP neurons, four showed an extended freqSTP while three showed an extended ampSTP (Fig. 11B). The electrophysiological fingerprint of the remaining 7 cells showed either exclusively a sustained outward rectification (2 out of 7) or exclusively an inward rectification (5 out of 7), and therefore could not be classified as a putative OT or AVP neuron and thus were not used in the analysis of phenotype. Overall the results suggest that the variation in the time course of STP following HFS is not a consequence of the neuronal phenotype of the postsynaptic cell.

It was then thought that the two responses, either the extended freqSTP or the extended ampSTP could be arising as a consequence of the stimulation protocol used to deliver the HFS since both 50 Hz (1 s, once) and 100 Hz (1 s, 2 times) had been employed. Though no detectable differences were seen between these two conditions when examining the overall frequency and amplitude responses, these analyses did not

rule out the possibility that the extended responses (extended freqSTP or extended ampSTP) could be arising as a consequence of one or the other stimulation protocols. However, it appeared that both extended freqSTP and extended ampSTP were seen using both types of stimulation protocols: 3 out of 10 cells in the 50 Hz condition showed an extended freqSTP, 4 out of 10 showed a extended ampSTP (Fig. 11C); 6 out of 11 cells in the 100 Hz condition had an extended freqSTP, 4 out of 11 had an extended ampSTP (Fig. 11D). From this it was concluded that the type of stimulation protocol used did not affect whether the cell responds with an extended freqSTP or an extended ampSTP.

3.7: The Postsynaptic Calcium is not Required for the Induction or Expression of STP

Removal of external calcium altogether completely blocked STP, including both the extended freqSTP as well as the extended ampSTP, meaning both responses depend on calcium entry (Fig. 12 and 13). Therefore, the next goal was to determine the locus of the calcium requirement, specifically the role of NMDA-receptor activation, as well as postsynaptic calcium. In order to test the dependence of either extended freqSTP or extended ampSTP on NMDA receptors, the NMDA receptor antagonist D-AP5 (25 μM) was bath applied for 20 minutes prior to stimulation. HFS in the presence of D-AP5 resulted in STP of both frequency and amplitude of mEPSCs to a similar extent as control (Fig. 14A and B; n = 4 and 11 for D-AP5 and control, respectively), with 1 out of 4 cells showing an extended freqSTP and 3 out of 4 showing an extended ampSTP.

Similarly, inclusion of EGTA (10 mM) in the recording pipette to chelate postsynaptic calcium also resulted in STP of both frequency and amplitude to a similar extent as a whole-cell control group (Fig. 14C and D; n = 4 and 7 for EGTA and control, respectively). In addition, both extended freqSTP and extended ampSTP were seen in this condition, with 3 out of 4 cells showing an extended freqSTP and 1 out of 4 showing an extended ampSTP, lending support to the fact that STP of either frequency or amplitude is unlikely to be due to a change in postsynaptic calcium. These pharmacological manipulations strongly suggest that neither the amplitude nor the frequency response require calcium signaling in the postsynaptic neuron, but instead result from changes occurring at the presynaptic terminal given that extracellular calcium was necessary for STP.

3.8: Kinetics of Large mEPSCs

Thus far it has been found that STP has two components, frequency and amplitude, and that these components have their own distinct time courses, both of which arise as a consequence of changes at the presynaptic terminal. The variation in the duration of these changes among cells does not depend on the phenotype of the postsynaptic cell or the stimulation protocol used. As part of this thesis project, an attempt to determine the mechanism behind the extended ampSTP was undertaken.

Changes in the kinetics of mEPSCs can indicate various changes happening at synapses and possibly help explain the increase in mEPSC amplitude that was seen. For example, it has been shown that as localized synaptic transmission is induced via

stimulation at sites progressively distal from the soma, mEPSCs become smaller, with slower rise times (Bekkers and Stevens, 1996). On the other hand, changes in the decay time of EPSCs can signify a change in the rate of transmitter clearance from the synaptic cleft or changes in the kinetics of postsynaptic receptors, both of which could result in larger mEPSCs (Stern, et al., 2000; Edmonds et al., 1995). To determine whether the large mEPSCs arising following HFS had different kinetics, mEPSCs were separated into groups according to three different criteria. The first group was comprised of mEPSCs before HFS, of which over 85% were 20 pA or less (control). The second group was comprised of mEPSCs post-HFS which were present after frequency returned to baseline and were no larger than 20 pA (late-post HFS small). The third group was also comprised of mEPSCs post-HFS which were present after frequency had returned to baseline but were 40 pA or greater (late post-HFS large). Differences in 10-90% rise times were observed between the groups (Fig. 15A; $p < 0.05$; one-way repeated measures ANOVA; $n = 8$) and it was found that the late large mEPSCs had faster rise times than the mEPSCs during control (Fig. 15A; $p < 0.02$; students paired t-test; $n = 8$). In contrast no detectable differences were observed in the rate of decay in the three groups outlined above (Fig. 15B). This suggests that the mEPSCs with larger amplitude and faster rise times occurring late post-HFS may be arising from the activation of previously inactive synapses more proximal to the postsynaptic neuron.

3.9: Sustained Amplitude Increase and Multiquantal Transmitter Release

Analysis of the amplitude distribution histograms from cells with an extended ampSTP revealed that 4 out of 8 cells clearly showed the presence of multiple peaks late post HFS when frequency had returned to baseline. This is highly indicative of multiquantal transmitter release. Figure 16 is an example of a cell showing this effect. In contrast, the other 4 cells which did not show apparent multiple peaks looked more similar to the example shown in Figure 10. In addition, one of the four cells in the EGTA condition and one of the four from the D-AP5 condition also showed multiple peaks, suggesting that this phenomenon is not at the locus of the postsynaptic cell. Given that this phenomenon is seen in every cell immediately post-HFS (Kombian et al., 2000) it is plausible that the multiple peaks we see in the amplitude distribution histograms of the extended ampSTP arise from the same mechanism, just at a later timepoint.

CHAPTER 4

DISCUSSION

4.1: Summary

The present work supports previous findings (Kombian et al., 2000) that HFS of excitatory afferent inputs to the SON induces a STP of both mEPSC frequency and amplitude. Miniature EPSC frequency increases 30-40 fold following stimulation while amplitude increases to about 140% of control.

Responses between cells were variable in both magnitude and duration. It was found that both the frequency and the amplitude of mEPSCs before stimulation were negatively related to their percent increase after stimulation, indicating that the greater the initial value, the smaller the level of potentiation, as would be expected. In contrast, the initial magnitude of STP (both frequency and amplitude) was positively correlated with how long each response persisted. Comparisons between the duration of freqSTP and ampSTP revealed that the time courses between the two parameters were not related, supporting the idea of two independent forms of synaptic plasticity triggered by the HFS. Cells were grouped according to the duration of the amplitude and frequency responses: a majority of cells were grouped as mEPSC amplitude response being longer than that of the frequency or vice versa, while a smaller group of cells had similar time courses. Analysis of the former two groups revealed that the discrepancies were arising independently of phenotype, stimulation protocol employed, NMDA receptors, and postsynaptic calcium. The fact that both freq- and ampSTP were not abolished by a

postsynaptic calcium chelator, together with the observation that removal of extracellular calcium prevents induction of STP, strongly suggests that the locus of plasticity is at the presynaptic terminal.

The kinetics of the mEPSCs were examined both before HFS and upon recovery of freqSTP, in an effort to explore possible mechanistic changes. It was found that the rise times in the large mEPSCs which were sustained after frequency had returned to baseline were faster than small mEPSCs that appeared during the same time frame or during the control period.

4.2: Frequency Increase Following HFS is Robust

With mEPSC frequency, a very large and obvious response to HFS is seen. It was previously determined that the frequency response consists of two phases, the first of which has a large amplitude and fast decay, the second becoming apparent successive to the first and decaying much more gradually (Quinlan et al., 2008). The initiation of the frequency response relies on calcium entry into the presynaptic terminal through high voltage activated calcium channels, while its prolonged duration of increase has been attributed to mitochondrial calcium sequestration and release (Quinlan et al., 2008). In the present investigation it was found that the degree of the initial increase following stimulation is related to how long the response persists. This could be related to the amount of calcium entering the presynaptic terminal and its subsequent sequestration into the mitochondria.

4.3: Amplitude Increase is Independent of Frequency Increase

AMPA-receptor mediated EPSCs in AVP and OT cells are known to have some distinct characteristics. It was previously shown that AMPA-receptor mediated mEPSC amplitude is lower and has a longer decay time in AVP neurons in comparison to OT neurons, which are characterized by larger mEPSCs that have a faster decay (Burnashev, 1996; Stern et al. 1999). Also, Hirasawa et al. (2003) had previously found that AVP had two distinct effects on AMPA-induced currents in the SON. On AVP neurons, AVP caused a decrease in evoked EPSCs and AMPA-induced currents, while it facilitated these same currents in OT neurons. For this reason, one of the first lines of investigation was to determine if either the OT or AVP neuron was more prone to respond with either a longer frequency change or a longer amplitude change. The possibility existed that presynaptic terminals impinging on AVP or OT neurons had different properties that manifest as distinct durations of amp- and freqSTP in response to HFS. However, in electrophysiologically identified AVP and OT cells this was not the case and that phenotype of MCNs is not a factor in the different responses to HFS.

4.4: Synaptic Plasticity of mEPSCs vs. Evoked EPSCs

Panatier et al. reported a long-term potentiation (LTP) of the amplitude of evoked EPSCs in the SON by using an intense HFS somewhat similar to our current study, i.e. 100 Hz, 1 sec, 4 times applied in current clamp mode (Panatier et al., 2006). Evoked EPSC-LTP is dependent on NMDA receptor activation and postsynaptic calcium

(Panatier et al., 2006). In this thesis, a holding potential of -80 mV was used for all of the experiments, which would prevent the activation of NMDA receptors on the postsynaptic cell. To eliminate the possibility that NMDA receptors on neighboring cells that are activated during HFS can somehow signal to modulate the excitatory synapses under investigation, the NMDA receptor antagonist D-AP5 was bath applied and it was found to have no effect on the amplitude increase of mEPSCs during STP. Furthermore, EGTA in the recording pipette also failed to block the amplitude response, a condition that has been shown to block evoked EPSC-LTP. Collectively, it is clear that the amplitude component of mEPSC-STP is not a byproduct of evoked EPSC-LTP but is a form of synaptic plasticity in its own right with a distinct mechanism of induction.

4.5: Amplitude Increase and Presynaptic Change

Conventionally, changes in mEPSC frequency have been attributed to changes occurring presynaptically, while changes in mEPSC amplitude have been attributed to postsynaptic change. This study challenges this idea, as the large amplitude mEPSCs we see in response to HFS seem to be arising from the presynaptic terminal. This is evident from two experimental results. Firstly, removal of extracellular calcium completely abolished any response to HFS, and secondly, inclusion of EGTA in the recording pipette and hence the postsynaptic cell failed to block the response, though it should be mentioned that EGTA is a slow acting, high capacity calcium chelator, and therefore, the speed of EGTA chelation may not completely remove the influence of postsynaptic calcium. However, several studies have also found changes in mEPSC amplitude as a

result of presynaptic changes in several brain areas such as the hippocampus (Tong and Jahr, 1994; Liu et al., 1999), cultured cortical neurons (Prange and Murphy, 1999), the cerebellum (Auger et al., 1998; Llano et al, 2000), and the PVN of the hypothalamus (Gordon and Bains, 2005).

Gordon and Bains (2005) have shown at excitatory synapses onto MCNs in the PVN that noradrenaline (NA) induces a rapid and robust increase in mEPSC amplitude which persisted for 10 to 20 minutes and then decreased to a new but elevated mean of 20% greater than baseline. This was due to activation of α_1-adrenoceptors and occurred independently of postsynaptic calcium which can cause AMPA-receptor insertion (Gordon and Bains, 2005). It is possible that in this thesis, the HFS used to stimulate glutamatergic afferents to the SON is also stimulating NAergic afferents. It is known that viscerosensory input is conveyed to the SON predominantly by NAergic fibers from the nucleus tractus solitarius and ventrolateral medulla which has a strong role in modulating the hypothalamic-pituitary-adrenal axis (Rinaman, 2007). Because there is most likely a variation in the density of NA afferents and the direction of their inputs to each MCN, it is reasonable to concede that some cells recorded in this study may receive more noradrenergic afferents than others. Furthermore, the positioning of the stimulating electrode relative to the recorded cell was not uniform. These discrepancies may possibly account for the variation in amplitude response between cells. Future studies could evaluate this possibility with an α_1-adrenoceptor antagonist.

4.6: Mechanism Behind the Amplitude Increase in mEPSCs

The amplitude increase immediately following HFS in the SON was previously suggested to be a result of multiquantal transmitter release, which is defined as the synchronization of transmitter release from multiple vesicles, and this was due to the fact that amplitude distribution histograms of the data revealed the presence of multiple equidistant peaks (Kombian et al., 2000). This was also found in the experiments in this thesis. Given that mEPSC frequency is so high during this time point, large numbers of quanta are being released as a consequence of abundant calcium entry into the presynaptic terminal (Quinlan et al., 2008). However, in about half of our cells, there are still large mEPSCs seen even at a later time point when mEPSC frequency has diminished. Some of these also show the presence of multiple peaks in amplitude distribution histograms suggesting that this is also due to multiquantal release. In the case of the large amplitude mEPSCs seen in response to NA application in the PVN, the authors also found this to be arising as a consequence of multiquantal transmitter release occurring for tens of minutes following the brief NA application (Gordon and Bains, 2005). They attribute this response to presynaptic endoplasmic reticulum calcium stores and show that extracellular calcium is not required (Gordon and Bains, 2005). The endoplasmic reticulum (ER) calcium store is filled during neuronal activity and serves as a calcium reservoir. Calcium release from the ER is known to contribute to presynaptic calcium transients and enhance spontaneous neurotransmitter release in some synapses (Llano et al., 2000; Emptage et al., 2001). Thus, at the SON synapse, it is possible that this calcium source could function in the potentiation of amplitude, even though it was

found to have no effect on the frequency (Quinlan et al., 2008). In addition, it is possible that the mitochondria, which were shown to be responsible for generating the second phase of the frequency increase during STP (Quinlan 2008), may be responsible for the persisting amplitude increase via storage and subsequent release of calcium.

Though multiquantal transmitter release seems quite plausible as the mechanism behind the amplitude increase, these larger mEPSCs also showed faster rise times. It has been shown that as localized synaptic transmission is induced via stimulation at sites progressively distal from the soma mEPSCs become smaller, with slower rise times (Bekkers and Stevens, 1996). This suggests that these larger mEPSCs could have also been caused by the activation of a previously silent proximal synapse, or by the strengthening of a proximal synapse that was only weakly active. However, if it is the activation of a silent synapse, it would also be expected that the frequency would be somewhat enhanced. As frequency has returned to baseline levels, making any definitive conclusions regarding the change in rise times that are seen should be done with caution. There could be calcium-independent changes occurring which could involve the switching of receptor subunits at the postsynaptic membrane. More work needs to be done to investigate the faster rise times seen in these experiments before any conclusions can be made.

4.7: Other Possibilities

Though evidence has been found here to suggest that the larger mEPSCs could be due to some combination of multiquantal transmitter release and activation of proximal

synapses, other factors may account for this response as well. Variability in the number of transmitter molecules in a vesicle would also cause a change in the response to a quantum (Liu, 2003). Activity levels have been shown to cause homeostatic changes in the presynaptic filling of both glutamatergic and GABAergic vesicles in cultured neurons (Hartman et al 2006; Wilson et al 2005). In this thesis however, this idea has not been investigated and therefore this possibility cannot be ruled out.

It is also possible that the persistent amplitude increase could also be a result of the synchronizing of transmitter release from multiple release sites following stimulation, a phenomenon called spatial summation. This is quite unlikely, however. In the analysis of amplitude, only those mEPSCs that had a smooth rise from baseline to peak were included. In order for spatial summation to account for the amplitude increase, quanta from multiple synapses to the same MCN would have to be released at a precise time point, down to the submillisecond. Given that by the time frequency returns to baseline, mEPSCs are only occurring at 1-2 Hz, so the likelihood of this happening so frequently and consistently between cells is low.

The idea that the persistent increase in size of the mEPSCs was due to a reduction in glutamate clearance leading to increases in ambient glutamate was also considered. This has been seen in instances such as when glial processes are withdrawn from around the neurons in the SON (Oliet, et al., 2001) and also in the case of multiquantal transmitter release (Gordon and Bains, 2005). However, if removal of glutamate occurs at a slower rate from the synapse, this likely would have been associated with a slower decay of the mEPSC (Edmonds et al., 1995). As there was no change in the decay rate of the

mEPSCs, the likelihood of the persistent amplitude increase arising from a reduction in transmitter clearance is also low.

4.8: Conclusion and Physiological Relevance

In these experiments, the differing time courses of the mEPSC frequency potentiation and amplitude potentiation in response to HFS suggests that these are two separate forms of synaptic plasticity. The frequency response has been well characterized previously, but here it is also revealed that the amplitude potentiation is not merely a by-product of the frequency response, but rather its own unique form of plasticity.

More needs to be clarified with reference to the mechanism behind the amplitude potentiation. Here some of the possibilities have been highlighted. Since preliminary data suggests that both multiquantal transmitter release as well as proximal synapse activation could be occurring, it is possible that there are multiple mechanisms involved in generating this response. Attention should be paid to NAergic signaling, while other investigations could seek to clarify the role of internal calcium stores in the presynaptic terminal. The endoplasmic reticulum and/or mitochondrial calcium could be causing long term effects on mEPSC amplitude.

Given that individual mEPSCs have been shown to be capable of generating action potentials, and that the MCNs of the SON have very high input resistances, small increases in excitation manifested as a doubling in size of mEPSCs in these neurons could have a large effect on MCN activity and influence hormonal release. Therefore the

amplitude potentiation which has been revealed here is likely a physiologically relevant form of synaptic plasticity and warrants further investigation.

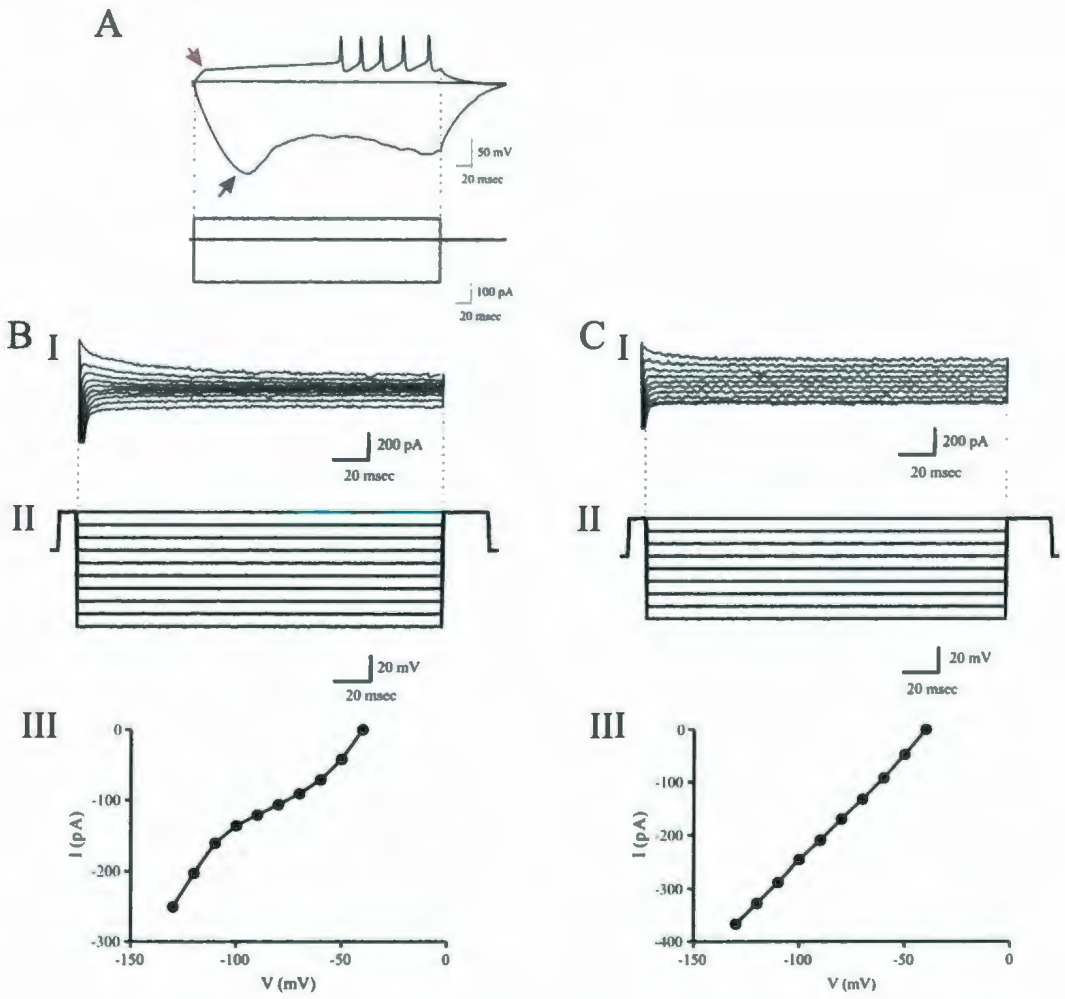

Figure 1: MCNs have distinct electrophysiological properties. A) Current clamp trace from a representative MCN showing the characteristic electrophysiological distinctions of I_A-current (red arrow) and I_H-current (blue arrow). Current protocol is indicated below with dotted lines marking start and end times of the protocol on the trace. B) Distinguishing characteristics of putative OT neurons. I) Voltage-clamp trace from a representative putative OT neuron showing sustained outward rectification and inward rectification in response to hyperpolarizing voltage steps (II), yielding a sigmoidal I-V relationship on an I-V plot (III). Data points are averages of 3 time points along the trace. C) Distinguishing characteristics of putative AVP neurons. I) Voltage-clamp trace from a representative putative AVP neuron showing no rectification to hyperpolarizing voltage steps (II) yielding a linear I-V relationship shown on I-V plot (III).

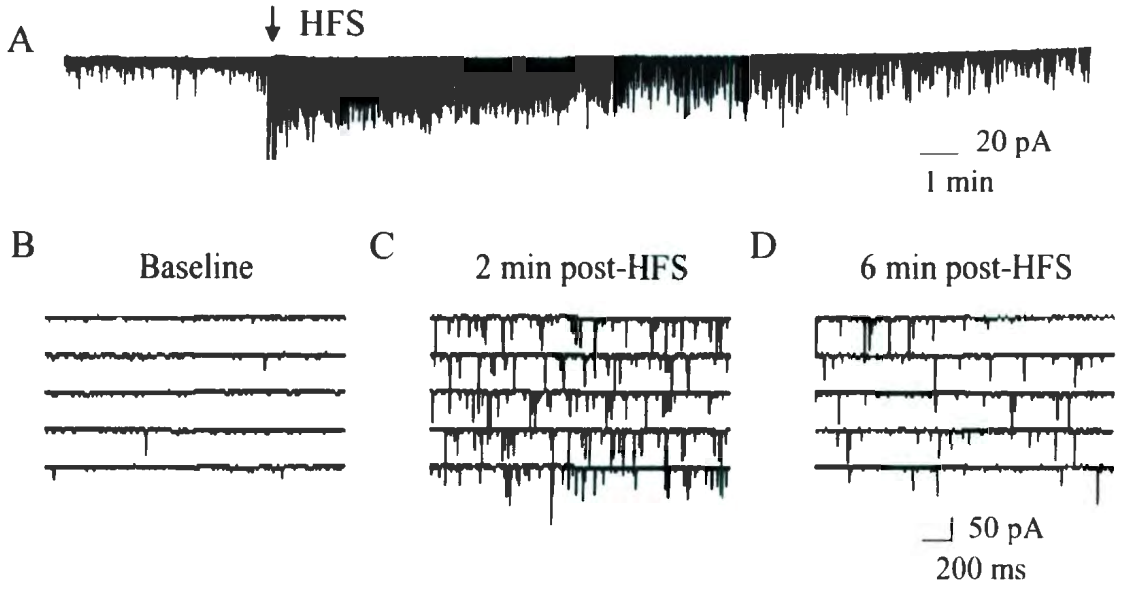

Figure 2: Short-term potentiation (STP) in the SON. A)Voltage-clamp trace from a representative cell held at -80 mV shows that HFS (50 Hz for 1 s) of the excitatory afferents to the SON results in potentiation of mEPSCs which persists for several minutes. Arrow denotes time of HFS delivery. B, C, & D) Expanded voltage clamp traces from the same cell as above illustrate the frequency and amplitude of mEPSCs during the control period, 2 minutes following and 6 minutes following HFS.

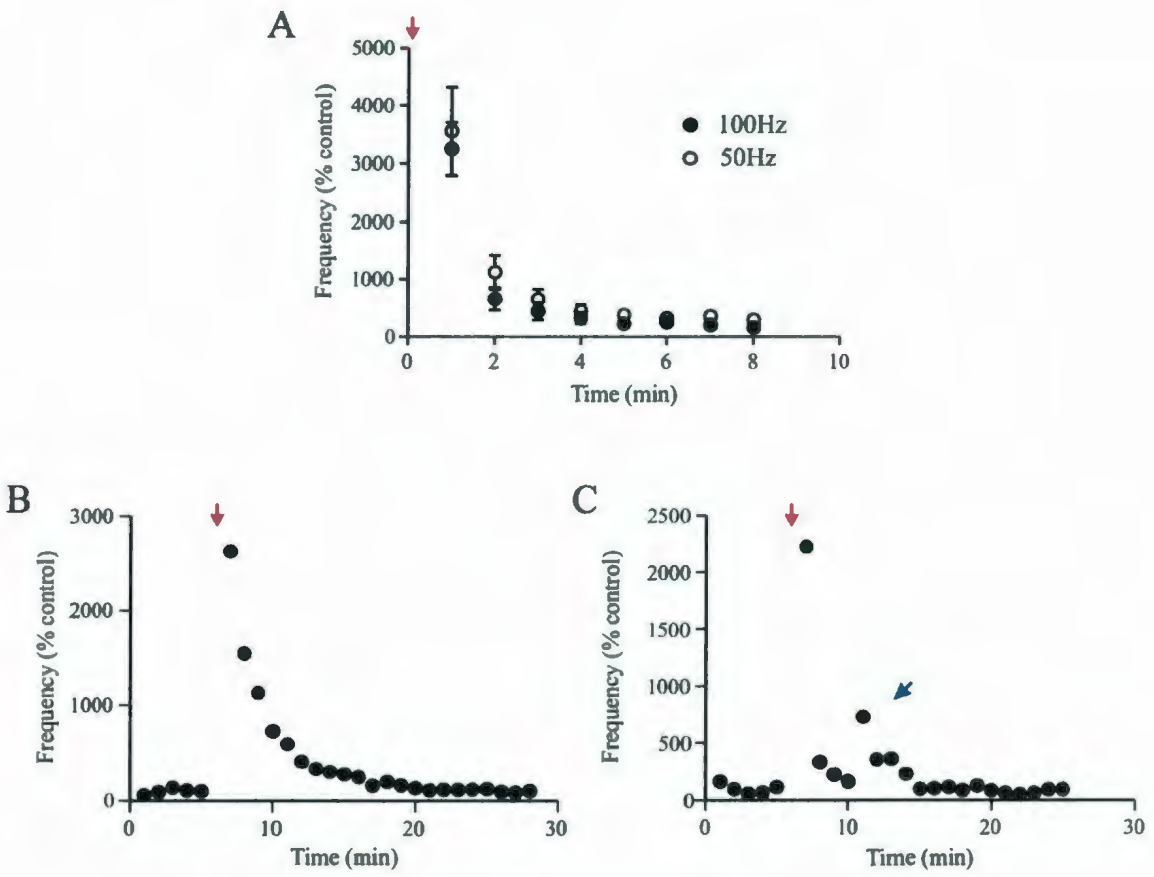

Figure 3: HFS to excitatory afferents to SON resulted in a robust increase in mEPSC frequency. A) Time-effect plot for overall frequency shows that a 50 Hz stimulus once for 1 s or a 100 Hz stimulus twice for 2 s results in a statistically similar increase in mEPSC frequency which decays exponentially (HFS given at time zero; n = 21; arrow denotes time of stimulation). B & C) Time-effect plots from two representative MCNs show that two patterns of mEPSC frequency increase are seen at this synapse. The first response (B) is characterized by an inital increase followed by a smooth decay back to baseline, while the second response (C) shows a second peak following the initial increase immediately following HFS, denoted by blue arrow. Red arrows indicate time of stimulation.

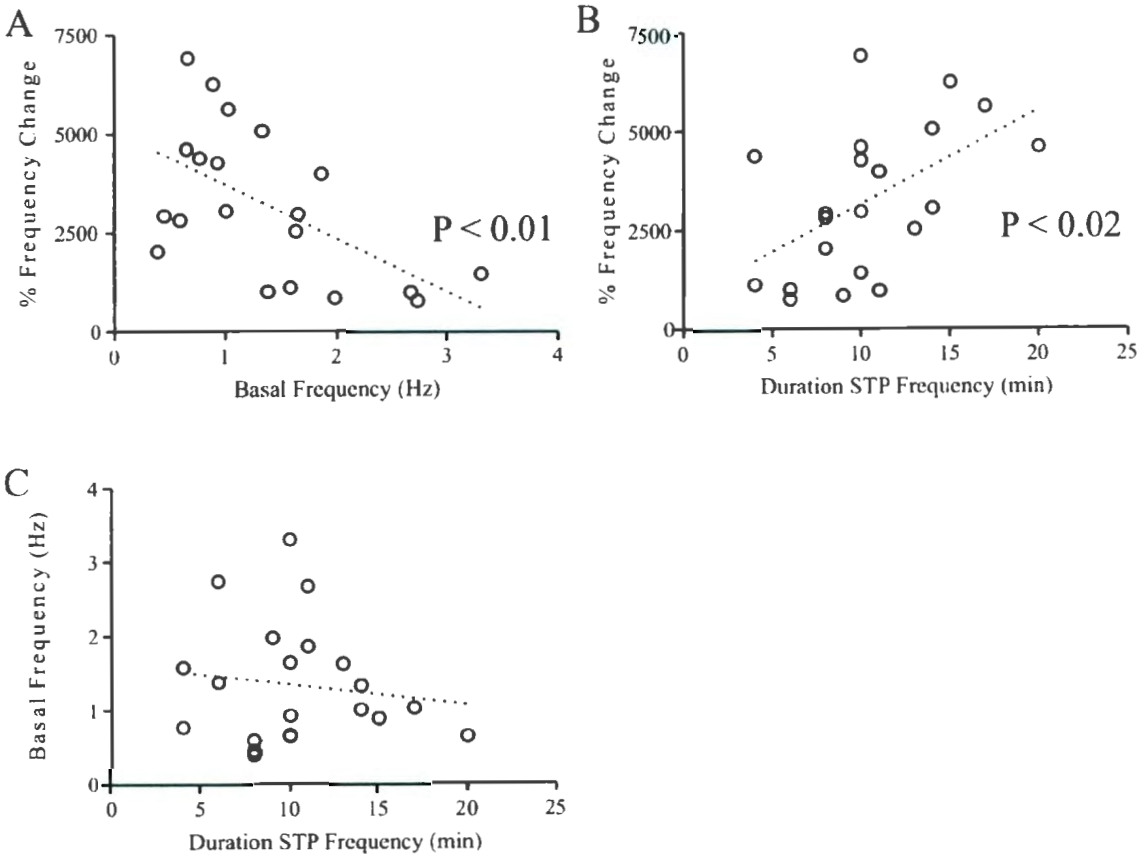

Figure 4: Basal mEPSC frequency affects the response to HFS. A) Scatter-plot with linear regression analysis reveals that the basal mEPSC frequency is negatively related to the percent change of frequency to HFS ($p < 0.01$; $n = 21$; each circle denotes a single MCN). B) Scatterplot showing that the percent change of mEPSC frequency is positively correlated to how long the response lasts ($p < 0.02$; $n = 21$). C) Scatter-plot showing that there is no direct relationship between basal mEPSC frequency to the duration of the response to HFS. Dotted lines signify the line of best fit.

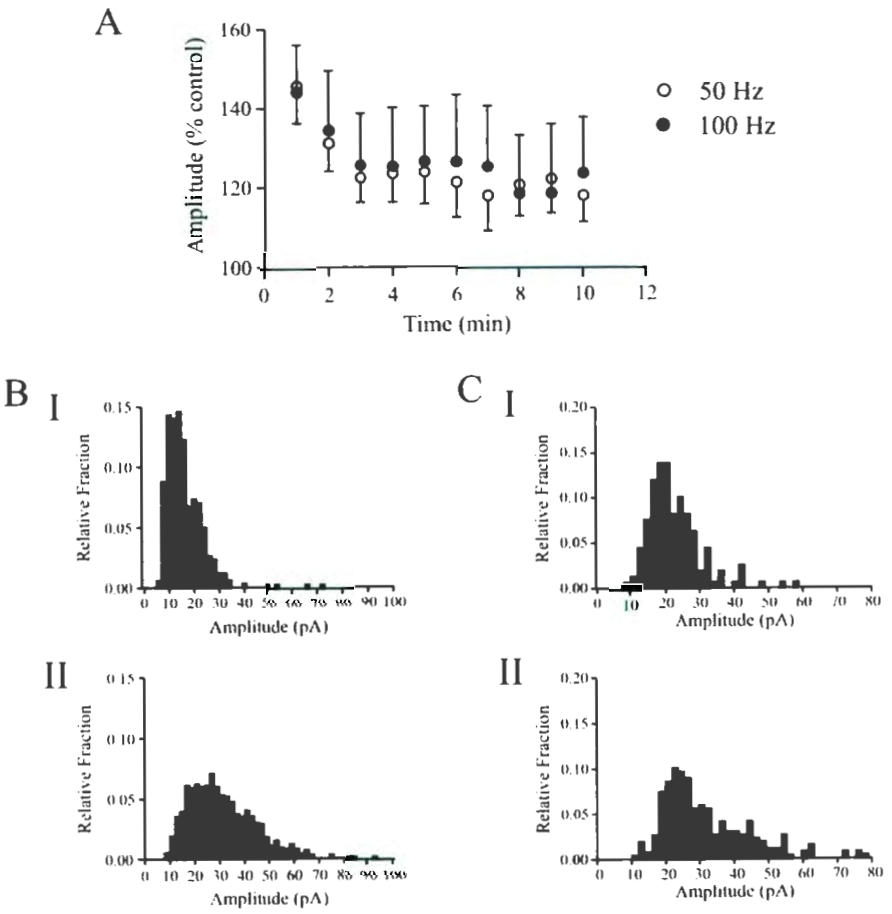

Figure 5: HFS to excitatory afferents results in an increase in mEPSC amplitude. A) Time-effect plot of amplitude shows that a 50 Hz stimulus once for 1 s or 100 Hz twice for 2 s results in a statistically similar increase in mEPSC amplitude which gradually approaches baseline (HFS given at time zero). B & C) Amplitude distribution histograms from two representative MCNs reveal that over the course of 5 minutes before stimulation the majority of mEPSCs are between 15 and 25 pA (B-I and C-I). During the first minute immediately after HFS (B-II and C-II) there is an increase in the number of larger amplitude mEPSCs. In 76% of cells, amplitude histograms appeared to show multiple peaks immediately after HFS (C-II).

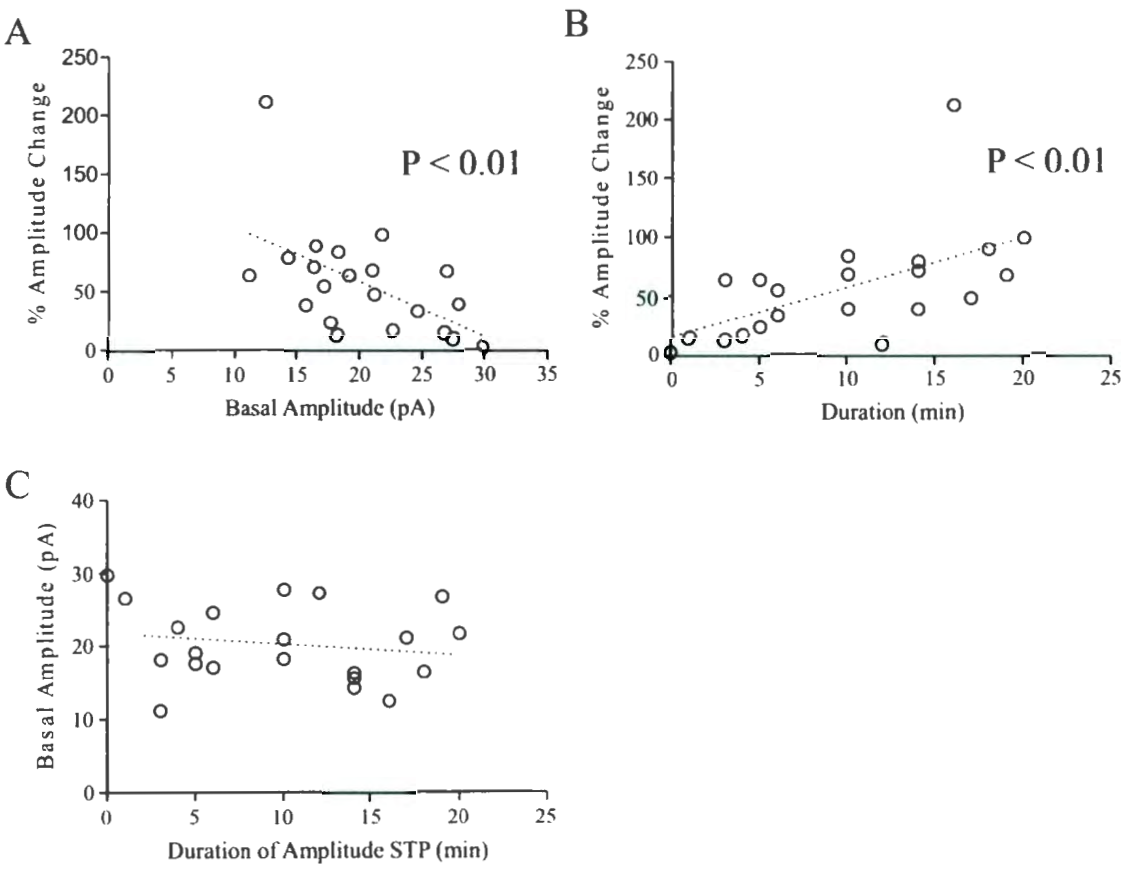

Figure 6: Basal mEPSC amplitude affects the response to HFS. A) Scatter-plot with linear regression analysis reveals that the basal mEPSC amplitude is negatively related to the percent change of amplitude to HFS ($p < 0.01$; $n = 21$; each circle denotes a single MCN). B) Scatterplot showing that the percent change of mEPSC amplitude is positively correlated to how long the response lasts ($p < 0.01$; $n = 21$). C) Scatter-plot showing that there is no direct relationship between basal mEPSC amplitude and the duration of the response to HFS. Dotted lines signify the line of best fit.

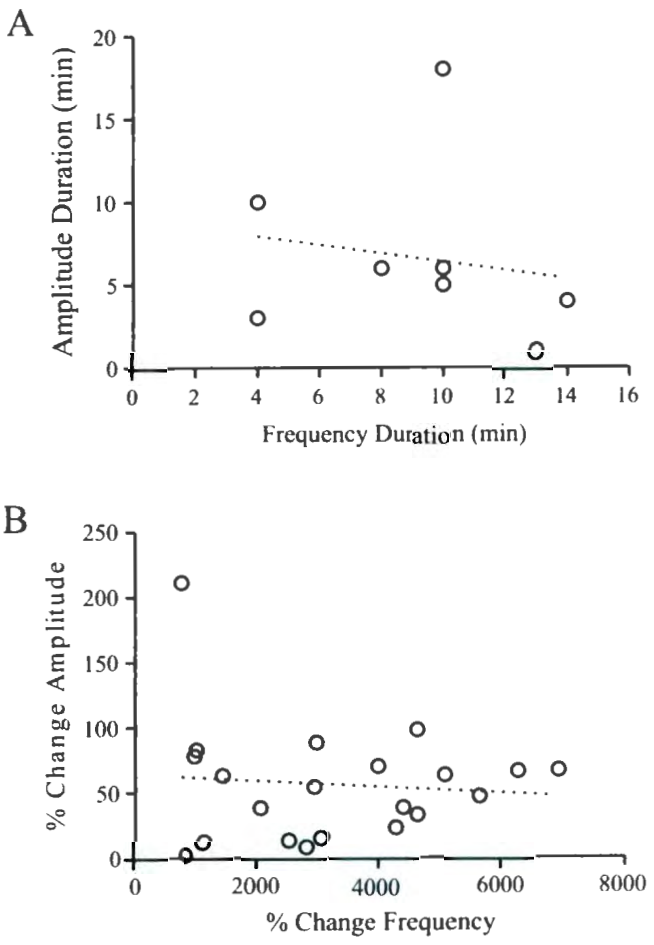

Figure 7: mEPSC frequency and amplitude increase following HFS are dissociated. A) Scatter-plot with linear regression analysis shows that the time courses of mEPSC frequency and amplitude increase following HFS are not related ($r^2 = 0.03263$; n = 8; each circle denotes a single MCN). B) Scatter-plot shows that the percent change of mEPSC frequency and amplitude are also not related ($r^2 = 0.01031$; n = 21). Dotted lines denote the line of best fit.

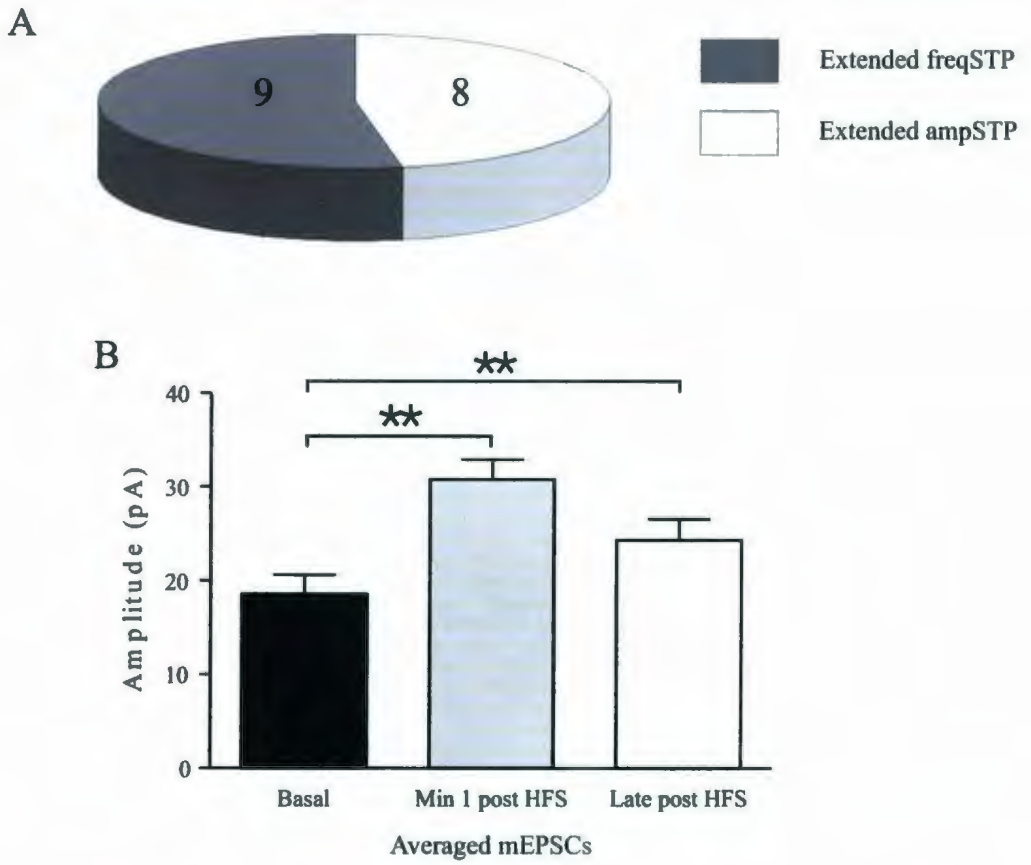

Figure 8: Dissociation of mEPSC frequency and amplitude enables an exclusive investigation of the amplitude increase without influence from the frequency increase. A) Pie chart showing that MCNs were divided into two groups based on differing time courses; 9 MCNs which showed a longer frequency change (extended freqSTP), and 8 MCNs which showed a longer amplitude change (extended ampSTP). B) Bar graph reveals that in the extended ampSTP group mEPSCs during the baseline were smaller than mEPSCs in the first minute post-HFS ($p < 0.01$; $n = 8$) as well as mEPSCs occurring when frequency had recovered ($p < 0.01$; $n = 8$).

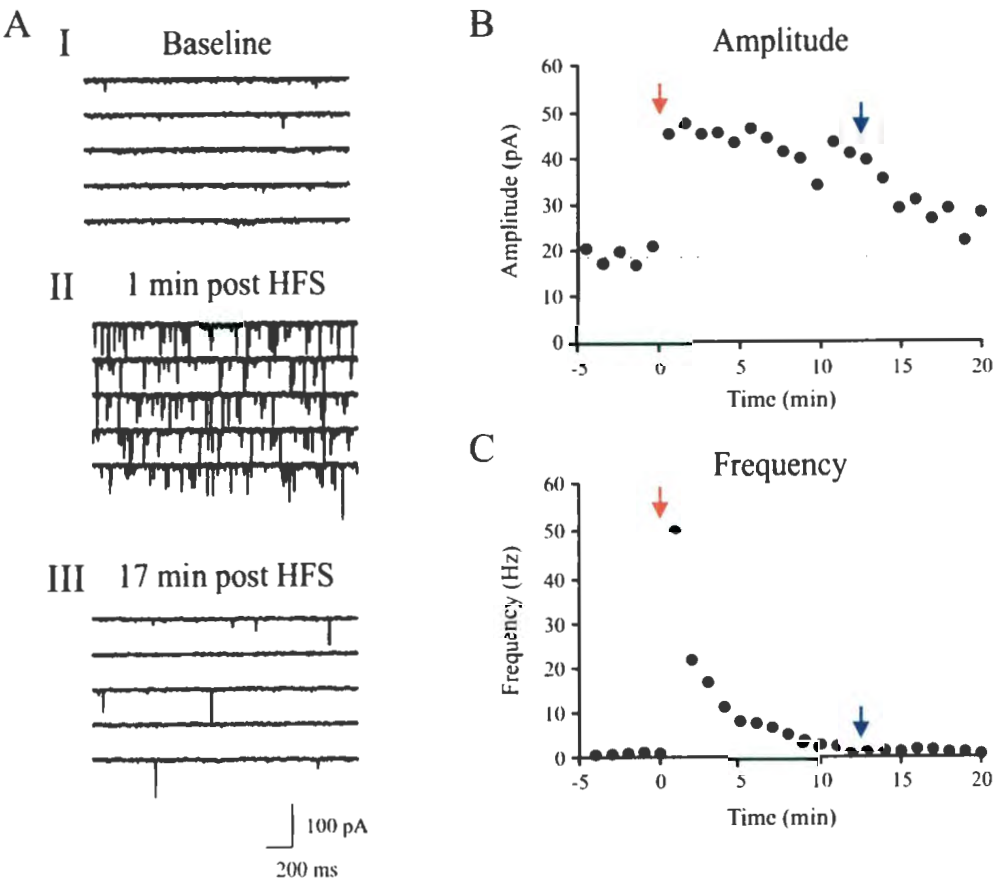

Figure 9: MCN showing an extended ampSTP. A) Voltage clamp traces taken from a representative MCN held at -80 mV during control (I), the first minute following HFS (II), and 5 minutes after frequency had returned to baseline level (III). B & C) Time-effect plots for both amplitude and frequency taken from the same cell as in (A). The red arrows indicate the time of stimulation while the blue arrows indicate the point when frequency is back to baseline.

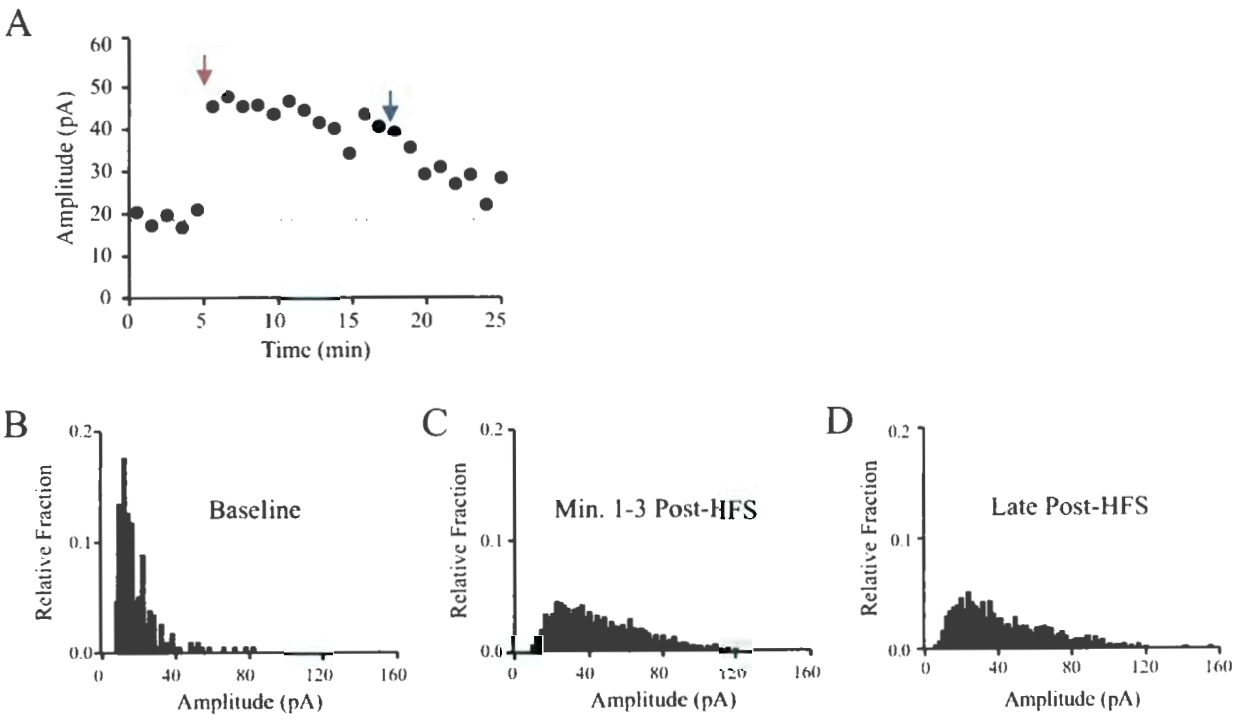

Figure 10: Amplitude histograms for the MCN shown in Figure 9. A) Time-effect plot of amplitude. The red arrow indicates time of stimulation, the blue arrow indicates the point where frequency has recovered. B, C, & D) Amplitude distribution histogram for mEPSCs during baseline (B), immediately following HFS (C), and when frequency has recovered (D). Before stimulation almost all of the events are between 10 and 20 pA, but after HFS about half of the events are between 40 and 80 pA and this increase is sustained even after frequency has returned to baseline.

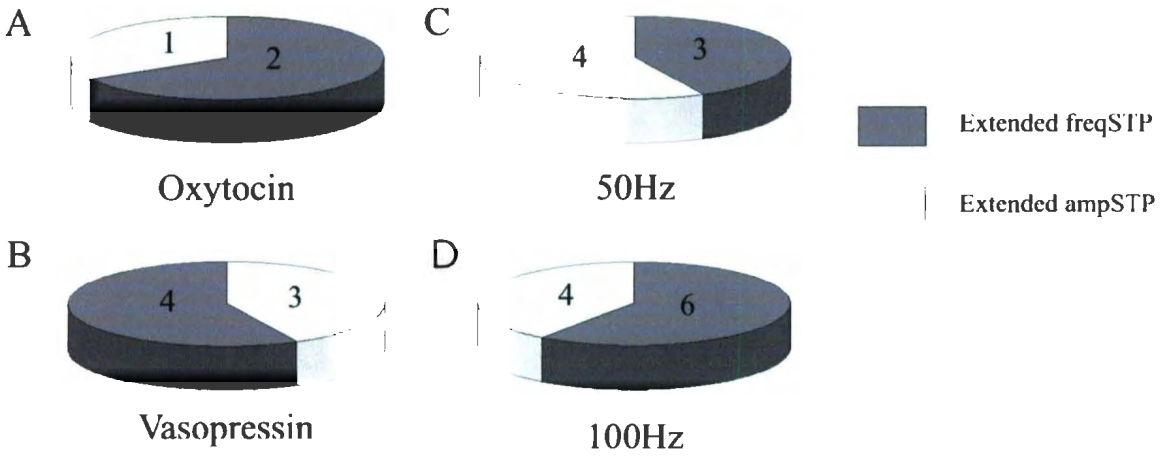

Figure 11: Whether a MCN expresses an extended freqSTP or an extended ampSTP does not depend on the phenotype of the MCN or the stimulation protocol employed. A & B) Both putative OT MCNs as well as putative AVP MCNs showed extended freqSTP and extended ampSTP. C & D) The type of response was independent of whether a 50 or 100 Hz stimulation protocol was used.

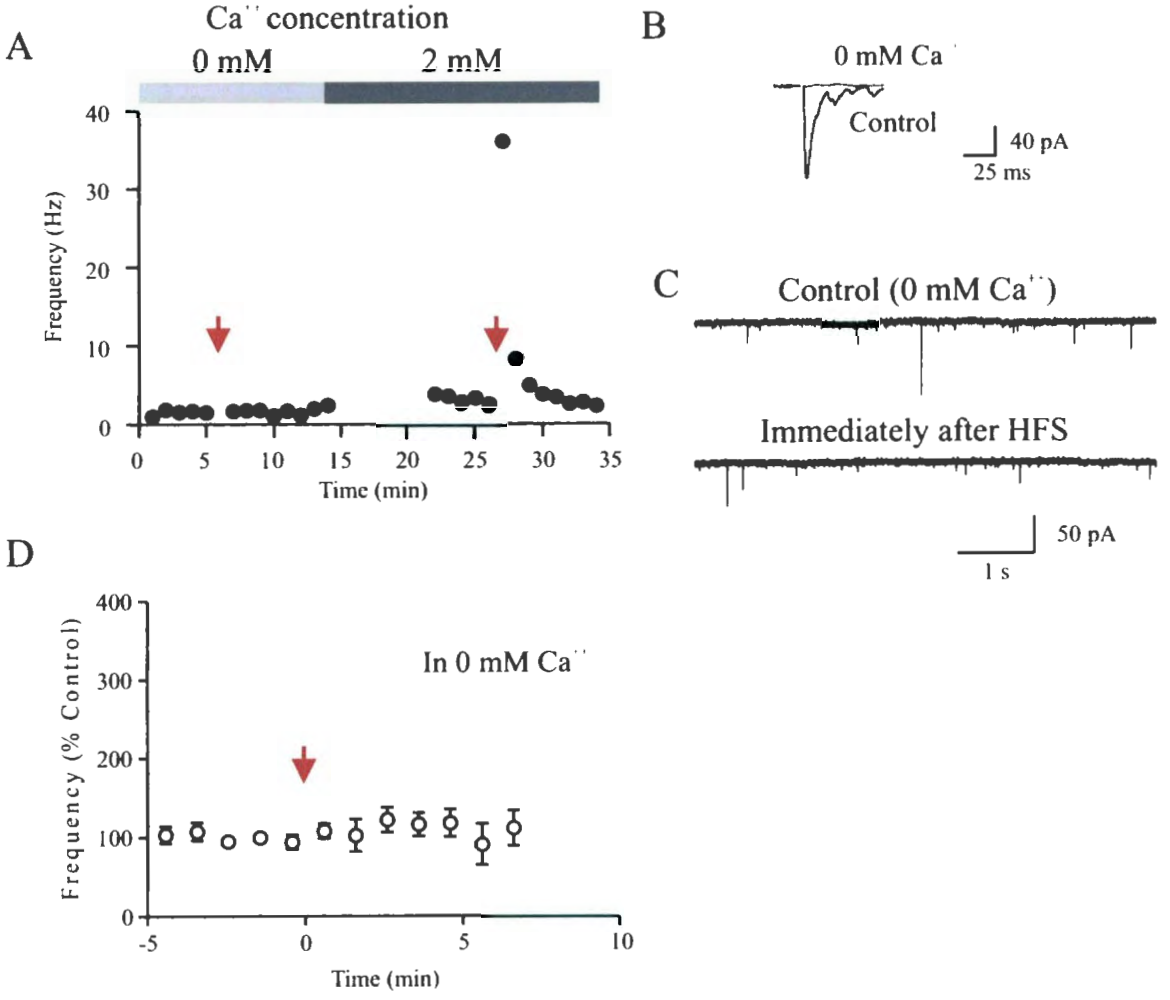

Figure 12: Removal of external calcium completely blocked the frequency increase after HFS. A) Time-effect plot of a representative MCN showing that in the absence of calcium mEPSC frequency does not increase in response to HFS. After 10 minute application of 2 mM calcium, STP occurred following HFS. B) Voltage clamp trace from a representative MCN shows that without calcium, the evoked response is blocked. C) Voltage clamp trace from a representative MCN in zero calcium before (top) and after HFS (bottom). D) Time effect plot of the overall group data (n = 5).

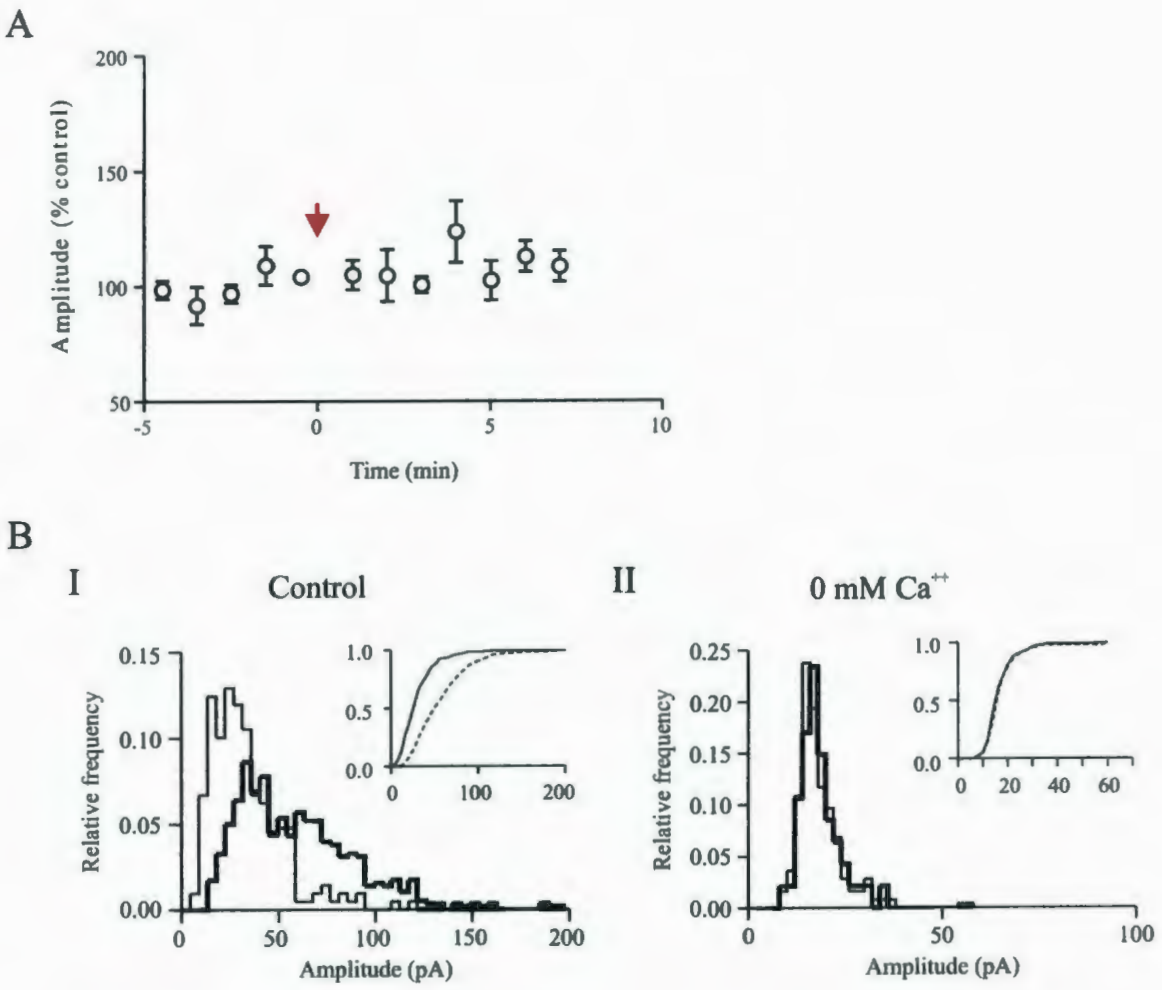

Figure 13: Removal of external calcium completely blocks the amplitude increase after HFS. A) Time-effect plot of amplitude showing that following HFS there is no response. The red arrow indicates time of stimulation. B) Distribution histograms showing the relative distribution of mEPSCs before (thin bar outline) and after (thick bar outline) HFS in control (I) and in the absence of calcium (II). Insets in top right corner show cumulative plot (solid line represents baseline; dashed line represents first minute after HFS).

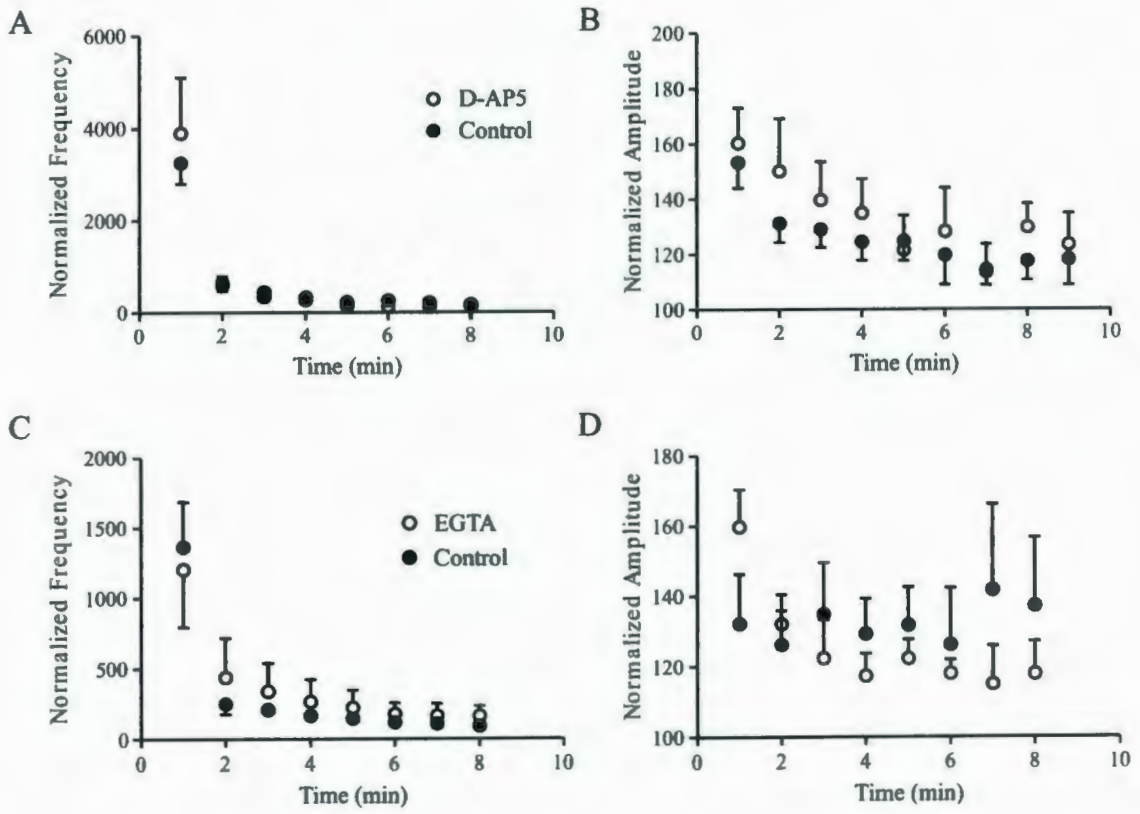

Figure 14: STP does not require NMDA receptors or postsynaptic calcium. A&B) Time-effect plots showing that bath application of D-AP5 did not block the frequency or amplitude increase to HFS (n=4 for D-AP5; n=11 for control). C&D) Time-effect plots showing that inclusion of 10mM EGTA in the recording pipette did not block the frequency or amplitude increase to HFS (n=4 for EGTA; n=5 for control).

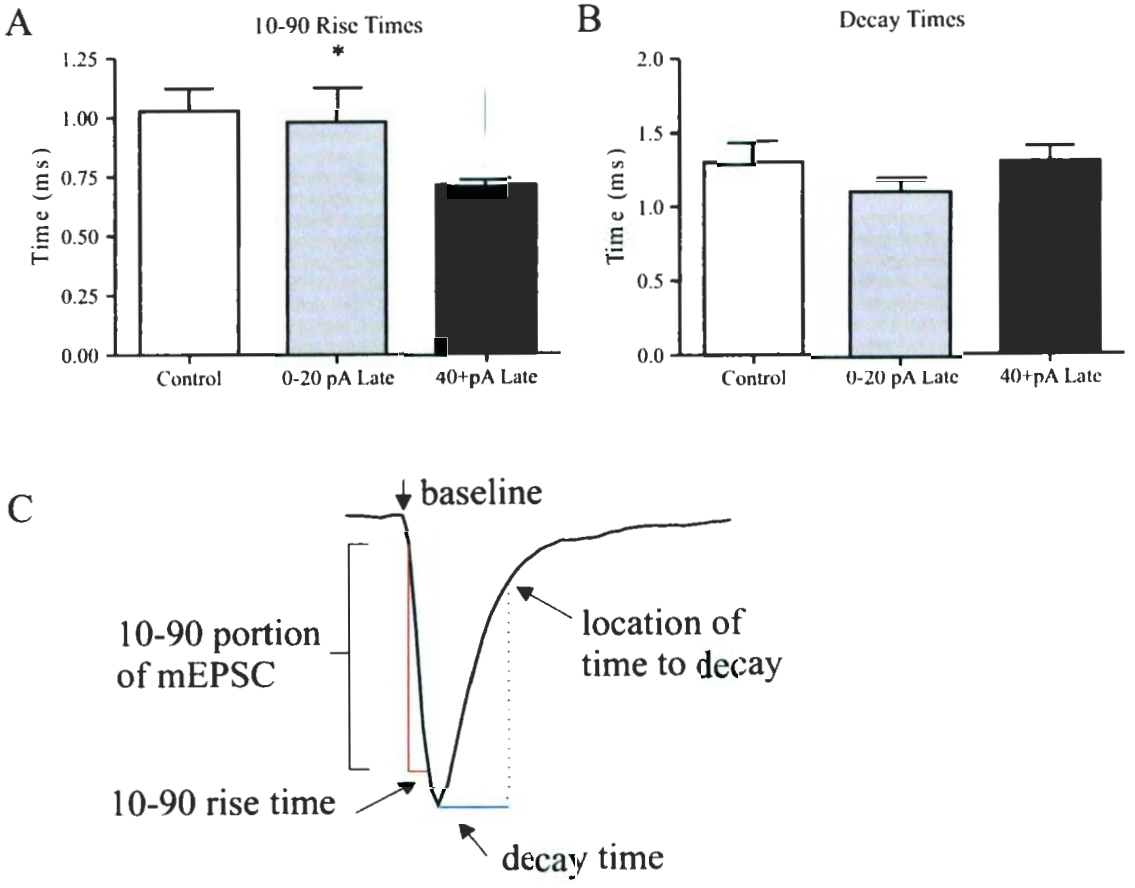

Figure 15: HFS-induced large mEPSCs have faster rise times. A) Comparison of 10-90% rise times shows that the large mEPSCs occurring once frequency recovers have faster rise times as compared to control ($n = 8$; $p < 0.05$). B) Bar graph showing there was no change in the decay time. C) Schematic of mEPSC illustrating how rise and decay times were generated.

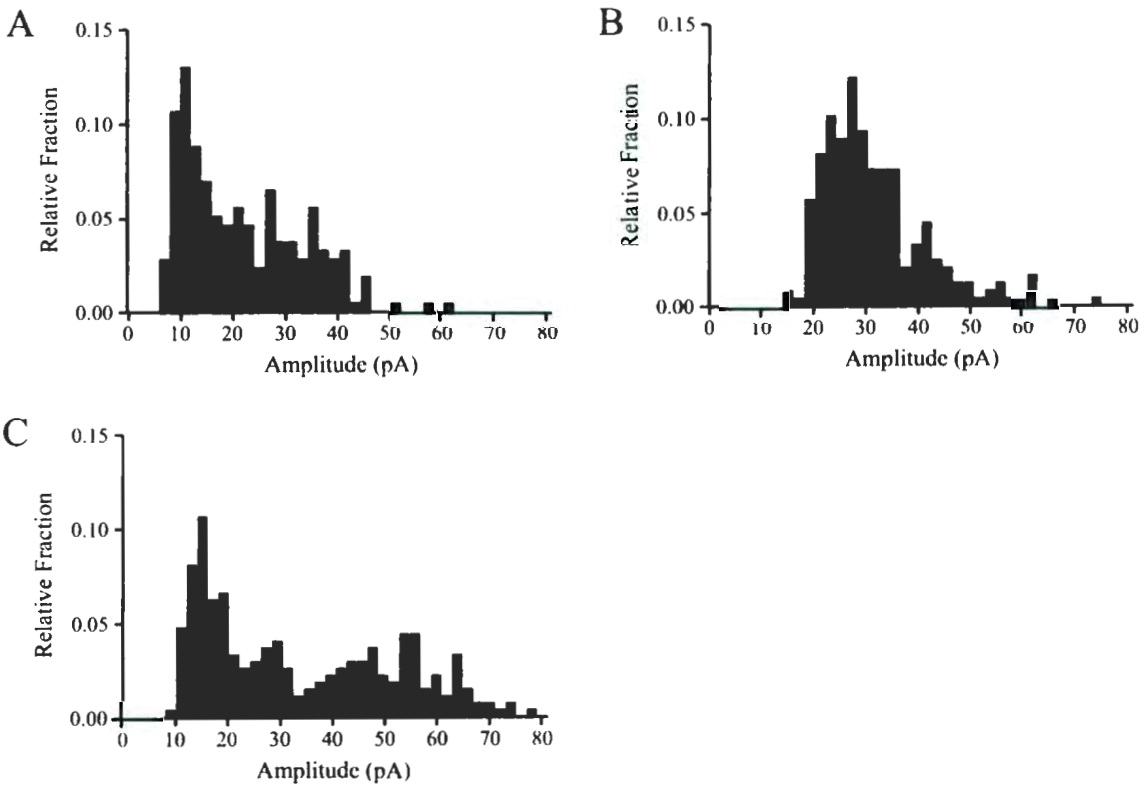

Figure 16: A fraction of the cells showing an extended ampSTP showed evidence of multiquantal transmitter release. A, B, & C) Amplitude distribution histograms show the different time points from a MCN during control (A), immediately following HFS (B), and once frequency had recovered, which clearly shows evidence of multiple peaks, indicative of multiquantal transmitter release (C).

REFERENCES

Adan RA, Van Leeuwen FW, Sonnemans MA , Brouns M, Hoffman G, Verbalis JG, and Burbach JP. (1995) Rat oxytocin receptor in brain, pituitary, mammary gland, and uterus: Partial sequence and immunocytochemical localization. *Endocrinology.* 136(9): 4022-4027.

Andrew RD and Dudek FE. (1983) Burst discharge in mammalian neuroendocrine cells involves an intrinsic regenerative mechanism. *Science.* 221: 1050-52.

Andrew RD and Dudek FE. (1984) Intrinsic inhibition in magnocellular neuroendocrine cells of rat hypothalamus. *J Physiol.* 353: 171-185.

Andrew RD, MacVicar B, Dudek R, and Hatton G. (1981) Dye transfer through gap junctions between neuroendocrine cells of the rat hypothalamus. *Science.* 211: 1187-1189

Antoni F. (1993) Vasopressinergic control of pituitary andrenocorticotropin secretion comes of age. *Front Neuroendocrinol.* 14: 76-122.

Aoyagi T, Birumachi J, Hiroyama M, Fujiwara Y, Sanbe A, Yamauchi J, and Tanoue A. (2007) Alteration of glucose homeostasis in V1a vasopressin receptor-deficient mice. *Endocrinology.* 148(5): 2075-84.

Armstrong WE. (1995) Morphological and electrophysiological classification of hypothalamic supraoptic neurons. *Prog Neurobiol.* 47:291–339.

Armstrong WE and Hatton GI. (2006) The puzzle of pulsatile oxytocin secretion during lactation: some new pieces. Am *J Physiol Regul Integr Comp Physiol.* 291: R26-R28.

Armstrong WE, Smith BN, and Tian M. (1994) Electrophysiological characteristics of immunochemically identified rat oxytocin and vasopressin neurones in vitro. *J Physiol.* 475(1): 115-128.

Auger C, Kondo S, Marty A (1998) Multivesicular release at single functional synaptic sites in cerebellar stellate and basket cells. *J Neurosci.* 18: 4532-4547

Barberis C, Mouillac B, and Durroux T. (1998) Structural bases of vasopressin/oxytocin receptor function. *J Endocrinol.* 156(2): 223-9.

Bekkers JM and Stevens CF. (1996) Cable properties of cultured hippocampal neurons determined from sucrose-evoked miniature EPSCs. ***J Neurophysiol.*** **75(3): 1250-5.**

Belin V, Moos F, Richard P. (1984) Synchronization of oxytocin cells in the hypothalamic paraventricular and supraoptic nuclei in suckled rats: direct proof with paired extracellular recordings. ***Exp Brain Res.*** **57:201–203.**

Bicknell RJ. (1988) Optimizing release from peptide hormone secretory nerve terminals. ***J Exp Biol.*** **139: 51–65.**

Bielsky IF, Hu SB, Szegda KL, Westphal H, and Young LJ. (2004) Profound impairment in social recognition and reduction in anxiety-like behavior in vasopressin V1a receptor knockout mice. ***Neuropsychopharmacology.*** **29: 483-493.**

Bisset GW and Fairhall KM. (1996) Release of vasopressin and oxytocin by excitatory amino acid agonists and the effect of antagonists on release by muscarine and hypertonic saline, in the rat in vivo. ***Br. J. Pharmacol.*** **117: 309-314.**

Blanks AM and Thornton S. (2003) The role of oxytocin in parturition. ***BJOG*** **110: 46-51.**

Bliss TVP and Collingridge GL. (1993) A synaptic model of memory: long-term potentiation in the hippocampus. ***Nature.*** **361: 31-19**

Boudaba C, Schrader LA, and Tasker JG. (1997) Physiological evidence for local excitatory synaptic circuits in the rat hypothalamus. ***J Neurophysiol.*** **77: 3396-3400**

Boudaba C and Tasker JG. (2006) Internuclear coupling of hypothalamic magnocellular nuclei by glutamate synaptic circuits. ***Am J Physiol Regul Integr Comp Physiol.*** **291: R102-R111.**

Bourque CW and Oliet SH. (1997) Osmoreceptors in the central nervous system. ***Ann Rev Physiol.*** **59: 601-619.**

Bourque CW, Kirkpatrick K, and Jarvis CR. (1998) Extrinsic modulation of spike afterpotentials in rat hypothalamoneurohypophysial neurons. ***Cell Mol. Neurobiol.*** **18, 3-12**

Brimble MJ and Dyball RE. (1977) Characterization of the responses of oxytocin- and vasopressin-secreting neurons in the supraoptic nucleus to osmotic stimulation. ***J Physiol.*** **271: 253-271.**

Brown CH, Bull PM, and Bourque CW (2004) Phasic bursts in rat magnocellular neurosecretary cells are not intrinsically regenerative in vivo. ***Eur J Neurosci.*** **19: 2977-2983**

Burbach JP, Hoop MJD, Schmale H, Richter D, Kloet ERD, Haaf JAT, and Wied DD. (1984) Differential responses to osmotic stress vasopressin-neurophysin mRNA in hypothalamic nuclei. ***Neuroendocrinology.*** **39: 582–584.**

Burnashev N. (1996) Calcium permeability of glutamate-gated channels in the central nervous system. ***Curr Opin Neurobiol.*** **6: 311-316.**

Conrad KP, Gellai M, North WG, and Valtin H. (1986) Influence of oxytocin on renal hemodynamics and electrolyte and water excretion. ***Am J Physiol Renal Fluid Electrolyte Physiol*** **251: F290–F296.**

Costa A, Yasin S, Hucks D, Forsling M, Besser G and Grossman A. (1992) Differential effects of neuroexcitatory amino acids on corticotropin-releasing hormone-41 and vasopressin release from rat hypothalamic explants. ***Endocrinology.*** **131: 2595-2602.**

Csaki A, Kocsis K, Kiss J, and Halasz B. (2002) Localization of putative glutamatergic/ aspartatergic neurons projecting to the supraoptic nucleus area of the rat hypothalamus. ***Eur J Neurosci.*** **16: 55-68.**

de Kock C, Burnashev N, Lodder J, Mansvelder H, and Brussaard A. (2004) NMDA receptors induce somatodendritic secretion in hypothalamic neurones of lactating female rats. ***J Physiol.*** **561(1): 53-64**

de Kock C, Wierda K, Bosman L, Min R, Koksma J, Mansvelder H, Verhage M, and Brussaard A. (2003) Somatodendritic secretion in oxytocin neurons is upregulated during the female reproductive cycle. ***Journal of Neuroscience.*** **23(7): 2726-2734**

Dudek FE and Gribkoff VK (1987) Synaptic activation of slow depolarization in rat supraoptic nucleus neurones in vitro. ***J Physiol.*** **387; 273-296**

Ebner K, Wotjak CT, Landgraf R, and Engelmann M. (2002) Forced swimming triggers vasopressin release within the amygdala to modulate stress-coping strategies in rats. ***Eur J Neuro.*** **15: 384-388.**

Edmonds B, Gibb AJ, and Colquhoun D. (1995) Mechanisms of activation of glutamate receptors and the time course of excitatory synaptic currents. ***Ann Rev.*** **57: 495-519.**

El Majdoubi M, Poulain DA, and Theodosis DT. (1996) The glutamatergic innervation of oxytocin- and vasopressin-secreting neurons in the rat supraoptic nucleus and its contribution to lactation-induced synaptic plasticity. ***J Neurosci.*** **8: 1377-1389**

El Majdoubi M, Poulain DA, and Theodosis DT. (1997) Lactation-induced plasticity in the supraoptic nucleus augments axodendritic and axosomatic GABAergic and glutamatergic synapses: an ultrastructural analysis using the dissector method. *Neuroscience.* 80: 1137-1147

Emptage NJ, Reid CA, and Fine A (2001) Calcium stores in hippocampal synaptic boutons mediate short-term plasticity, store-operated Ca2+ entry, and spontaneous transmitter release. Neuron 29, 197-208

Favaretto AL, Ballejo GO, Albuquerque-Araujo WI (1997) Oxytocin releases atrial natriuretic peptide from rat atria in vitro that exerts negative ionotropic and chronotropic action. *Peptides.* 18: 1377-1381.

Febo M, Numan M, and Ferris CF. (2005) Functional magnetic resonance imaging shows oxytocin activates brain regions associated with mother–pup bonding during suckling. *J Neurosci.* 25(50): 11637-11644.

Gimpl G and Fahrenholz F. (2001) The oxytocin receptor system: structure, function, and regulation. *Physiol Rev.* 81: 629-683.

Gordon GR and Bains JS. (2005) Noradrenaline triggers multivesicular release at glutamatergic synapses in the hypothalamus. Journal of Neuroscience. 25(49): 11385-11395

Gould BR and Zingg HH. (2003) Mapping oxytocin receptor gene expression in the mouse brain and mammary gland using an oxytocin receptor-LacZ reporter mouse. *Neuroscience.* 122: 155-167.

Gribkoff VK and Dudek FE. (1990) Effects of excitatory amino acid antagonist on synaptic responses of supraoptic neurons in slices of rat hypothalamus. *J. Neurophysiol.* 63: 60-71.

Griebel G, Simiand J, Serradeil-Le Gal C, Wagnon J, Pascal M, Scatton B, Maffrand JP, and Soubrié P. (2002) Anxiolytic- and antidepressant-like effects of the non-peptide vasopressin V_{1b} receptor antagonist, SSR149415, suggest an innovative approach for the treatment of stress-related disorders. *Neurobiol.* 99(9): 6370-6375.

Gutkowska J, Jankowski M, Mukaddam-Daher S, and McCann SM. (2000) Oxytocin is a cardiovascular hormone. *Braz J Med Biol Res* 33: 625–633.

Hartman KN, Pal SK, Burrone J, and Murthy VN. (2006) Activity-dependent regulation of inhibitory synaptic transmission in hippocampal neurons. *Nat Neurosci.* 5: 642-649

Hatton GI (1997) Function-related plasticity in hypothalamus. *Annu Rev Neurosci.* 20; 375-397

Hatton GI, Ho YW, and Mason WT. (1983) Synaptic activation of phasic bursting in rat supraoptic nucleus neurones recorded in hypothalamic slices. *J Physiol.* 345: 297-317.

Hatton GI, Yang QZ, and Cobbett P. (1987) Dye coupling among immunocytochemically identified neurons in the supraoptic nucleus: increased incidence in lactating rats. *Neuroscience.* 21: 923-930

Hatton GI and Yang QZ. (2002) Synaptic potentials mediated by alpha 7 nicotinic acetylcholine receptors in supraoptic nucleus. *J Neurosci.* 22(1): 29-37

Hawrylak N, Fleming J, and Salm A. (1998) Dehydration and rehydration selectively and reversibly alter glial fibrillary acidic protein immunoreactivity in the rat supraoptic nucleus and subjacent glial limitans. *Glia.* 22: 260-271

Hirasawa M, Kombian SB, and Pittman QJ. (2001) Oxytocin retrogradely inhibits evoked, but not miniature, EPSCs in the rat supraoptic nucleus: role of N- and P/Q-type calcium channels. *J Physiol.* 532(3): 595-607

Hirasawa M, Mouginot D, Kozoriz M, Kombian SB, and Pittman QJ. (2003) Vasopressin differentially modulates non-NMDA receptors in vasopressin and oxytocin neurons in the supraoptic nucleus. *Journal of Neuroscience.* 23(10): 4270-4277

Hirasawa M, Schwab Y, Natah S, Hillard CJ, Mackie K, Sharkey KA, and Pittman QJ. (2004) Dendritically released transmitters cooperate via autocrine and retrograde actions to inhibit afferent excitation in rat brain. *J Physiol.* 559(2): 611-624

Hu B, Cunningham JT, Nissen R, Renaud LP, and Bourque CW. (1992) Rat supraoptic neurons are resistant to glutamate neurotoxicity. *Neuroreport.* 3(1): 87-90.

Hu B and Bourque CW (1992) NMDA receptor-mediated rhythmic bursting activity in rat supraoptic nucleus neurones in vitro. *J Physiol.* 458, 667-687

Inenaga K, Honda E, Hirakawa T, Nakamura S, and Yamashita H. (1998) Glutamatergic synapses to mouse supraoptic neurons in calcium-free medium in vitro. *J Neuroendocrinol.* 10: 1-7.

Iremonger KJ and Bains JS. (2007) Integration of asynchronously released quanta prolongs the postsynaptic spike window. *J Neurosci.* 27(25): 6684-6691.

Israel JM, Le Masson G, Theodosis DT, and Poulain DA. (2003) Glutamatergic input governs periodicity and synchronization of bursting activity in oxytocin neurons in hypothalamic organotypic cultures. ***Eur J Neurosci.*** **17: 2619-2629**

Jirikowski GF, Back H, Forssmann WG & Stumpf WE. (1986) Coexistence of atrial natriuretic factor (ANF) and oxytocin in neurons of the rat hypothalamus. ***Neuropeptides*****, 8: 243-249.**

Johnson AK and Gross PM. (1993) Sensory circumventricular organs and brain homeostatic pathways. ***FASEB J*** **7: 678–686.**

Jourdain P, Israel JM, Dupouy B, Oliet S, Allard M, Vitiello S, Theodosis DT, and Poulain DA. (1998) Evidence for a hypothalamic oxytocin-sensitive pattern-generating network governing oxytocin neurons in vitro. ***J Neurosci.*** **18(17): 6641-6649.**

Kabashima N, Shibuya I, Ibrahim N, Ueta Y, and Yamashita H. (1997) Inhibition of spontaneous EPSCs and IPSCs by presynaptic GABAB receptors on rat supraoptic magnocellular neurons. ***J Physiol.*** **504 (1):113-26.**

Kiss A and Mikkelsen JD. (2005) Oxytocin- anatomy and functional assignments: a minireview. ***Endocrine Regulations.*** **39: 97-105.**

Knepper MA. (1997) Molecular physiology of urinary concentrating mechanism: regulation of aquaporin water channels by vasopressin. ***Am J Physiol Renal Physiol.*** **272: F3-F12.**

Kombian SB, Hirasawa M, Matowe WC, and Pittman QJ. (2001) GABA(B) receptors modulate short-term potentiation of spontaneous excitatory postsynaptic currents in the rat supraoptic nucleus in vitro. *Neuropharmacol.* **41(5):554-64**

Kombian SB, Hirasawa M, Mouginot D, and Pittman QJ. (2002) Modulation of synaptic transmission by oxytocin and vasopressin in the supraoptic nucleus. ***Prog Brain Res.*** **139: 235- 246**

Kombian SB, Hirasawa M, Mouginot D, Chen X, and Pittman Q. (2000) Short-term potentiation of miniature excitatory synaptic currents causes excitation of supraoptic neurons. ***J Neurophysiol.*** **83: 2542-2553.**

Kombian SB, Mouginot D, and Pittman QJ. (1997) Dendritically released peptides act as retrograde modulators of afferent excitation in the supraoptic nucleus in vitro. ***Neuron.*** **19: 903-912.**

Lambert RC, Moos FC, and Richard P. (1993) Action of endogenous oxytocin within the paraventricular or supraoptic nuclei: a powerful link in the regulation of

the bursting pattern of oxytocin neurons during milk-ejection reflex in rats. *Neuroscience* 57: 1027–1038.

Langle S, Poulain D, and Theodosis D. (2003) Induction of rapid, activity-dependent neuronal-glial remodeling in the adult rat hypothalamus in vitro. *European Journal of Neuroscience.* 18: 206-214

Landgraf R and Neumann ID. (2004) Vasopressin and oxytocin release within the brain: a dynamic concept of multiple and variable modes of neuropeptide communication. *Front Neuroendocrinol.* 25: 150-176.

Li C, Tripathi PK, and Armstrong WE. (2007) Differences in spike train variability in rat vasopressin and oxytocin neurons and their relationship to synaptic activity. *J Physiol.* 581, 221-240

Lightman SL and Young WS III. (1987) Vasopressin, oxytocin, dynorphin, enkephalin and corticotrophin-releasing factor mRNA stimulation in the rat. *J Physiol* 394: 23–39.

Liu G. (2003) Presynaptic control of quantal size: kinetic mechanisms and implications for synaptic transmission and plasticity. *Curr Opin Neurobiol.* 13: 324-331

Liu G, Choi S, Tsien RW (1999) Variability of neurotransmitter concentration and nonsaturation of postsynaptic AMPA receptors at synapses in hippocampal cultures and slices. *Neuron.* 22: 395-409

Llano I, Gonzalez J, Caputo C, Lai FA, Blayney LM, Tan YP, and Marty A. (2000) Presynaptic calcium stores underlie large-amplitude miniature IPSCs and spontaneous calcium transients. *Nat Neurosci.* 3(12): 1256-1265

Lolait SJ, O'Carroll AM, and Brownstein MJ. (1995) Molecular biology of vasopressin receptors. *Ann NY Acad Sci* 771: 273–292.

Lolait SJ, O'Carroll AM, McBride OW, Konig M, Morel A, and Brownstein MJ. (1992) Cloning and characterization of a vasopressin V2 receptor and possible link to nephrogenic diabetes insipidus. *Nature.* 357: 336–339.

Ludwig M. (1998) Dendritic release of vasopressin and oxytocin. *J Neuroendocrinol.* 10: 881-895.

Ludwig M and Pittman QJ (2003) Talking back: dendritic neurotransmitter release. *Trends Neurosci.* 26, 255-261

Ludwig M, Bull P, Tobin V, Sabatier N, Landgraf R, Dayanithi G, and Leng G. (2005) Regulation of activity-dependent dendritic vasopressin release from rat supraoptic neurones. *Journal of Physiology*. 564(2): 515-522

Lynch MA. (2004) Long-term potentiation and memory. *Physiol Rev.* 84: 87-136.

McKinley MJ, Gerstberger R, Mathai ML, Oldfield BJ, and Schmid H. (1999) The lamina terminalis and its role in fluid and electrolyte homeostasis. *J Clin Neurosci* 6: 289–301.

Meeker RB, Greenwood RS, Hayward JN. (1994) Glutamate receptors in the rat hypothalamus and pituitary. *Endocrinology*. 134: 621-629

Meeker RB, Swanson DJ, Greenwood RS, and Hayward JN. (1993) Quantitative mapping of glutamate presynaptic terminals in the supraoptic nucleus and surrounding hypothalamus. *Brain Research.* 600: 112-122

Meister B, Cortes R, Villar MJ, Schalling M, and Hokfelt T. (1990) Peptides and transmitter enzymes in hypothalamic magnocellular neurons after administration of hyperosmotic stimuli : comparison between messenger RNA and peptide/protein levels. *Cell Tissue Res.* 260: 279-297.

Morel A, O'Carroll AM, Brownstein MJ, and Lolait SJ. (1992) Molecular cloning and expression of a rat V1a arginine vasopressin receptor. *Nature.* 356: 523–526.

Micevych R, Popper P, and Hatton G. (1996) Connexin-32 mRNA expression in rat supraoptic nucleus: up-regulation prior to parturition and during lactation. *Neuroendocrinology*. 63: 39-45

Miyata S, Nakashima T, and Kiyohara T. (1994) Expression of c-*fos* immunoreactivity in the hypothalamic magnocellular neurons during chronic osmotic stimulations. *Neurosci Lett* 175: 63–66.

Moos F, Fontanaud P, Mekaouche M, and Brown D. (2004) Oxytocin neurones are recruited into coordinated fluctuations of firing before bursting in the rat. *Neuroscience.* 125: 391-410

Moos F, Freund-Mercier MJ, Guerne Y, Guerne JM, Stoeckel ME and Richard P. (1984) Release of oxytocin and vasopressin by magnocellular nuclei in vitro: specific facilitatory effect of oxytocin on its own release. *J Endocrinol.* 102; 63-72

Nagatomo T, Inenaga K, and Yamashita H. (1995) Transient outward current in adult rat supraoptic neurones with slice patch-clamp technique: inhibition by angiotensin II. *J Physiol.* 485(1): 87-96.

Nemenoff RA. (1998) Vasopressin signaling pathways in vascular smooth muscle. *Front Biosci.* 15(3): d194-207.

Nielsen S, Chou CL, Marples D, Christensen EI, Kishore BK, and Knepper MA. (1995) Vasopressin increases water permeability of kidney collecting duct by inducing translocation of aquaporin-CD water channels to plasma membrane. *Proc Natl Acad Sci USA* 92: 1013–1017.

Nissen R, Bourque CW, and Renaud LP. (1993) Membrane properties of organum vasculosum lamina terminalis neurons recorded in vitro. *Am J Physiol.* 264(4 Pt 2): R811-815.

Nissen R, Hu B, and Renaud LP. (1995) Regulation of spontaneous phasic firing of rat supraoptic vasopressin neurones in vivo by glutamate receptors. *J Physiol. (Lond.)* 484: 415-424.

Nonoguchi H, Owada A, Kobayashi N, Takayama M, Terada Y, Koike J, Ujiie K, Marumo F, Sakai T, and Tomita K. (1995) Immunohistochemical localization of V2 vasopressin receptor along the nephron and functional role of luminal V2 receptor in terminal inner medullary collecting ducts. *J Clin Invest* 96: 1768–1778.

Oliet S, Piet R, and Poulain D. (2001) Control of glutamate clearance and synaptic efficacy by glial coverage of neurons. *Science.* 292: 923-926

Panatier A, Gentles SJ, Bourque CW, and Oliet SH. (2006) Activity-dependent synaptic plasticity in the supraoptic nucleus of the rat hypothalamus. *J Physiol.* 573(3): 711-21.

Poulain DA and Wakerley JB. (1982) Electrophysiology of hypothalamic magnocellular neurones secreting oxytocin and vasopressin. *Neuroscience.* 7: 773–808.

Prange O, Murphy TH (1999) Analysis of multiquantal transmitter release from single cultured cortical neuron terminals. *J Neurophysiol.* 81: 1810-1817

Quinlan ME, Alberto CO, and Hirasawa M. (2008) Short-term potentiation of mEPSCs requires N-, P/Q- and L-type Ca2+ channels and mitochondria in the supraoptic nucleus. *J Physiol.* 586(13):3147-61.

Raggenbass M. (2001) Vasopressin- and oxytocin-induced activity in the central nervous system: electrophysiological studies using in vitro systems. *Prog Neurobiol.* 64: 307-326.

Renaud LP and Bourque CW (1991) Neurophysiology and neuropharmacology of hypothalamic magnocellular neurons secreting vasopressin and oxytocin. *Prog Neurobiol.* 36:131–169.

Richard P, Moos F, and Freund-Mercier M. (1991) Central effects of OT. *Physiology Reviews.* 71: 331-370

Rinaman, L. (2007) Visceral sensory inputs to the endocrine hypothalamus. *Frontiers in Neuroendocrinology* 28: 50-60.

Roland BL and Sawchenko PE (1993) Local origins of some GABAergic projections to the paraventricular and supraoptic nuclei of the hypothalamus in the rat. *J Comp Neurol.* 332(1):123-43

Schrader LA and Tasker JG. (1997) Modulation of multiple potassium currents by metabotropic glutamate receptors in neurons of the hypothalamic supraoptic nucleus. *J Neurophys.* 78(6): 3428-3437.

Share L. (1988) Role of vasopressin in cardiovascular regulation. *Physiol Rev* 68: 1248–1284.

Shibata R, Nakahira K, Shibasaki K, Wakazono Y, Imoto K, and Ikenaka K (2000) A-type K^+ current mediated by the Kv4 channel regulates the generation of action potential in developing cerebellar granule cells. *J Neurosci.* 20: 4145-4155.

Shojo H and Kaneko Y. (2000) Characterization and expression of oxytocin and the oxytocin receptor. *Mol Genet Metab.* 71: 552–558.

Sladek CD, Badre SE, Morsette DJ, and Sidorowicz HE. (1998) Role of non-NMDA receptors in osmotic and glutamate stimulation of vasopressin release: effect of rapid receptor desensitization. *J Neuroendocrinol.* 10:897-903.

Sofroniew MV (1983) Direct reciprocal connections between the bed nucleus of the stria terminalis and dorsomedial medulla oblongata: evidence from immunohistochemical detection of tracer proteins. *J Comp Neurol.* 213(4):399-405.

Stern JE, Galarreta M, Foehring RC, Hestrin S, and Armstrong WE. (1999) Differences in the properties of ionotropic glutamate synaptic currents in oxytocin and vasopressin endocrine neurons. *J Neurosci.* 19: 3367-3375.

Stern JE, Hestrin S, and Armstrong WE. (2000) Enhanced neurotransmitter release at glutamatergic synapses on oxytocin neurons during lactation in the rat. *J Physiol.* 526(1): 109-114.

Stern JE and Armstrong WE. (1995) Electrophysiological differences between oxytocin and vasopressin neurones recorded from female rats in vitro. *J Physiol.* 488(3): 701-708.

Stricker EM and Verbalis JG. (1986) Interaction of osmotic and volume stimuli in the regulation of neurohypophyseal secretion in rats. ***Am J Physiol.*** **250: R267-275.**

Tasker JG and Dudek FE (1991) Electrophysiological properties of neurones in the region of the paraventricular nucleus in slices of rat hypothalamus. ***J Physiol.*** **434:271-93.**

Theodosis D, Trailin A, and Poulain D. (2006) Remodeling of astrocytes, a prerequisite for synapse turnover in the adult brain? ***Am J Physiol Regul Integr Comp Physiol.*** **290: R1175-R1182**

Thibonnier M, Auzan C, Madhun Z, Wilkins P, Berti-Mattera L, and Clauser E. (1994) Molecular cloning, sequencing, and functional expression of a cDNA encoding the human V1a vasopressin receptor. ***J Biol Chem*** **269: 3304–3310.**

Thibonnier M, Conarty DM, Preston JA, Plesnicher CL, Dweik RA, and Erzurum SC. (1999) Human vascular endothelial cells oxytocin receptors. ***Endocrinology*** **140: 1301–1309.**

Tong G, Jahr CE (1994) Multivesicular release from excitatory synapses of cultured hippocampal neurons. ***Neuron.*** **12: 51-59**

Tribollet E, Barberis C, Jard S, Dubois-Dauphin M, and Dreifuss JJ. (1988) Localization and pharmacological characterization of high affinity binding sites for vasopressin and oxytocin in the rat brain by light microscopic autoradiography. ***Brain Research.*** **442: 105–118.**

Uvnas-Moberg K. (1998) Antistress pattern induced by oxytocin. ***News Physiol Sci.*** **13: 22-26.**

Valenti G, Procino G, Tamma G, Carmasino M, and Svelto M. (2005) Minireview: aquaporin 2 trafficking. ***Endocrinology.*** **146(12): 5063-70.**

Verbalis JG. (1999) The brain oxytocin receptor(s)? ***Front Neuroendocrinol*** **20: 146–156.**

Wakerly JB and Noble R. (1983) Extrinsic control of phasic supraoptic neurons in vitro: burst initiation and termination following brief changes in excitatory drive. ***Neuroscience Letters.*** **42: 329-334.**

Wang YF and Hatton GI (2007) Dominant role of betagamma subunits of G-proteins in oxytocin-evoked burst firing. ***J Neurosci.*** **27(8):1902-12.**

Wilson NR, Kang J, Hueske EV, Leung T, Varoqui H, Murnick JG, Erickson JD, and Liu G. (2005) Presynaptic regulation of quantal size by the vesicular glutamate transporter VGLUT1. ***J Neurosci.*** **25: 6221-6234**

Windle RJ, Shanks N, Lightman SL, and Ingram CD. (1997) Central oxytocin administration reduces stress-induced corticosterone release and anxiety behavior in rats. ***Endocrinology.*** **138(7): 2829-2834.**

Wuarin, JP and Dudek FE. (1993) Patch-clamp analysis of spontaneous synaptic currents in supraoptic neuroendocrine cells of the rat hypothalamus. ***J. Neurosci.*** **13: 2323-2331.**

Xu-Friedman MA and Regehr WG. (2004) Structural contributions to short-term synaptic plasticity. ***Physiol Rev.*** **84: 69-85.**

Yamamoto T, Sasaki S, Fushimi K, Ishibashi K, Yaoita E, Kawasaki K, Marumo F, and Kihara I. (1995) Vasopressin increases AQP-CD water channel in apical membrane of collecting duct cells in Brattleboro rats. ***Am J Physiol Renal Fluid Electrolyte Physiol*** **268: F1546–F1551.**